

REPORT SERIES IN AEROSOL SCIENCE

N:o 273 (2024)

ENHANCED QUANTIFICATION OF URBAN BIOGENIC  
CARBON DIOXIDE EXCHANGE USING LAND SURFACE  
MODELLING

MINTTU HAVU

Institute for Atmospheric and Earth System Research / Physics  
Faculty of Science  
University of Helsinki  
Helsinki, Finland

*Doctoral dissertation, to be presented for public discussion with the permission of the  
Faculty of Science of the University of Helsinki, in Auditorium E204, Physicum, on  
the 19th of January, 2024 at 13 o'clock.*

**Aerosolitutkimusseura r.y.**

**Helsinki 2024**

Author's Address: Institute for Atmospheric and Earth System Research  
P.O. Box 64  
FI-00014 University of Helsinki  
minttu.havu@helsinki.fi

Supervisors: Professor Leena Järvi, Ph.D.  
Institute for Atmospheric and Earth System Research  
University of Helsinki

Liisa Kulmala, Ph.D.  
Finnish Meteorological Institute

Professor Timo Vesala, Ph.D.  
Institute for Atmospheric and Earth System Research  
University of Helsinki

Reviewers: Professor Eeva-Stiina Tuittila, Ph.D.  
School of Forest Sciences  
Faculty of Science, Forestry and Technology  
University of Eastern Finland

Olli Peltola, Ph.D.  
Natural Resources Institute Finland (LUKE)

Opponent: Professor Lucy Hutyra, Ph.D.  
Department of Earth and Environment  
Boston University

ISBN 978-952-7507-23-0 (printed version)

ISSN 0784-3496

Helsinki 2024

Unigrafia Oy

ISBN 978-952-7507-24-7 (pdf version)

ISSN 2814-4236

Helsinki 2024

<http://www.FAAR.fi>

## Acknowledgements

I want to start by expressing my gratitude for my supervisors Professor Leena Järvi, Liisa Kulmala and Professor Timo Vesala. Their guidance, assistance, and encouraging words have been invaluable. My journey started as a summer worker over six years ago in the Urban meteorology group and Leena has been my supervisor since. Leena, I want to express my gratitude for your belief in me, the priceless insights into urban meteorology, and the opportunities to explore the world. Liisa, I want to thank you for your deep insights and unending enthusiasm for urban soils. I've gained a wealth of knowledge from your guidance. Timo, I wish to thank you not only for your support but also for sharing your passion for atmospheric sciences and creating a welcoming and cooperative working community.

The research presented in this thesis was conducted at the Institute for Atmospheric and Earth System Research (INAR), University of Helsinki. I thank Academician Markku Kulmala, the director of INAR, for providing the supportive work environment and the essential infrastructure. I also wish to acknowledge the financial support by Tiina and Antti Herlin Foundation. I thank Professor Eeva-Stiina Tuittila and Olli Peltola for reviewing my thesis, and Professor Lucy Hutyra for agreeing to be my opponent. I thank all my co-authors for their contributions, and special thanks to Yingqi and Michael for their peer support and collaborative efforts regarding the model simulations.

I want to express my appreciation to the entire Urban meteorology group for creating a relaxed and supportive working environment, making this journey much more enjoyable. Our shared coffee breaks and the Monday Cake Club together, alongside the Micrometeorology group, have truly been invaluable. I also extend my thanks to my colleagues and fellow meteorology study friends for their peer support and lunch breaks. It's been a pleasure sharing this journey with all of you.

Finally, I wish to express my deepest gratitude to my family for their unwavering support. To my parents, sister, and all my family members, thank you for your constant encouragements. I must give a special thanks to our dog, who has been the best antidote to stress during this process. Lastly, I want to thank my husband, Miika, for standing by me and supporting my goals and dreams.

Minttu Havu

Helsinki, December 2023

Minttu Pauliina Havu

University of Helsinki, 2024

## **Abstract**

Cities aiming for carbon neutrality encounter considerable challenges, as urban areas are major contributors of carbon dioxide (CO<sub>2</sub>) to the atmosphere. Besides reducing emissions, cities are determined to increase their CO<sub>2</sub> sinks. Urban emissions can be estimated based on fossil fuel consumption or atmospheric observations, where the role of urban vegetation has remained unclear. This knowledge gap arises from the lack of suitable assessment methods. This thesis aims to improve the modelling capabilities and assess the role of biogenic CO<sub>2</sub> exchange in relation to anthropogenic emissions for two key reasons: 1) Biogenic components introduce uncertainties in monitoring anthropogenic emissions, and 2) urban vegetation and soil can offset a part of these emissions.

This thesis focuses on estimating biogenic CO<sub>2</sub> components in urban areas at various scales using the urban land surface model SUEWS and the soil carbon model Yasso. For this purpose, both biogenic and anthropogenic CO<sub>2</sub> exchanges are implemented into SUEWS. The developed CO<sub>2</sub> module, particularly its biogenic part, is evaluated against eddy covariance observations in Helsinki and Beijing, and, together with the Yasso model, against street tree measurements in Helsinki. This thesis extends the use of the CO<sub>2</sub> module to city-wide simulations in Helsinki and projects CO<sub>2</sub> exchange with the RCP8.5 scenario for the 2050s.

The thesis extends the application of biogenic CO<sub>2</sub> components from individual street trees to neighbourhood and city-wide simulations. The main findings of the thesis are as follows: 1) SUEWS effectively simulates CO<sub>2</sub> exchange at both neighbourhood and street tree scales. 2) When estimating CO<sub>2</sub> exchange of urban vegetation, it is critical to also consider soil. 3) The biogenic CO<sub>2</sub> sinks in Helsinki are almost equally divided between extensive urban forests and neighbourhoods, and are projected to increase by 11% in response to climate change, due to an extended growing season, even though CO<sub>2</sub> uptake decreases during the summer months. 4) The proportion of net CO<sub>2</sub> exchange attributed to biogenic components varies at the neighbourhood and city scales, being approximately 7% in Helsinki.

This thesis not only advances our understanding of urban CO<sub>2</sub> dynamics but also emphasizes the vital role of urban green in offsetting anthropogenic emissions. The findings have broad implications for urban planning, stressing the importance of incorporating green infrastructure for sustainable and resilient cities in the face of a changing climate.

Keywords: urban, carbon dioxide, land surface model, soil carbon, vegetation, climate change

# Contents

<b>1</b>	<b>Introduction</b>	<b>5</b>
<b>2</b>	<b>Surface-atmosphere interactions</b>	<b>9</b>
2.1	Urban boundary layer . . . . .	9
2.2	Urban net CO <sub>2</sub> exchange . . . . .	11
2.3	Empirical quantification of CO <sub>2</sub> and water exchanges . . . . .	13
<b>3</b>	<b>Materials and methods</b>	<b>18</b>
3.1	Sites and measurements . . . . .	18
3.1.1	Helsinki . . . . .	19
3.1.2	Beijing . . . . .	20
3.2	CO <sub>2</sub> modelling . . . . .	22
3.2.1	SUEWS . . . . .	22
3.2.2	Yasso . . . . .	26
3.3	Forcing data . . . . .	27
3.4	Surface characteristics . . . . .	27
3.5	Local Climate Zones (LCZs) . . . . .	28
3.6	Statistics . . . . .	28
<b>4</b>	<b>Results</b>	<b>30</b>
4.1	Model evaluation . . . . .	30
4.1.1	Neighbourhood-scale . . . . .	30
4.1.2	Street trees and soil . . . . .	33
4.1.3	Applicability of SUEWS for simulating urban CO <sub>2</sub> exchange . . . . .	36
4.2	CO <sub>2</sub> exchange of street tree plantings . . . . .	37
4.3	Impact of surface cover on biogenic CO <sub>2</sub> exchange in a changing climate . . . . .	39
4.4	Offset of biogenic CO <sub>2</sub> exchange . . . . .	41
<b>5</b>	<b>Conclusions</b>	<b>44</b>
<b>6</b>	<b>Review of papers and the author’s contribution</b>	<b>47</b>
	<b>References</b>	<b>49</b>

## List of publications

This thesis consists of an introductory review, followed by four research articles. **Paper I** is reprinted under the Creative Commons Attribution-NonCommercial-NoDerivatives 4.0 International (CC BY-NC-ND 4.0), **Papers II** and **III** under the Creative Commons Attribution 4.0 International (CC BY 4.0), and **Paper IV** is reprinted with the permission from Elsevier. In the introductory part, these papers are cited according to their roman numerals.

- I** Järvi, L., **Havu, M.**, Ward, H.C., Bellucco, V., McFadden, J.P., Toivonen, T., Heikinheimo, V., Kolari, P., Riikonen, A., and Grimmond, C.S.B. (2019). Spatial modeling of local-scale biogenic and anthropogenic carbon dioxide emissions in Helsinki. *J. Geophys. Res. Atmos.*, 124:8363–8384, DOI: 10.1029/2018JD029576
- II** **Havu, M.**, Kulmala, L., Kolari, P., Vesala, T., Riikonen, A., and Järvi, L. (2022). Carbon sequestration potential of street tree plantings in Helsinki. *Biogeosciences*, 19(8):2121–2143, DOI: 10.5194/bg-19-2121-2022
- III** Zheng, Y., **Havu, M.**, Liu, H., Cheng, X., Wen, Y., Lee, H.S., Ahongshangbam, J., and Järvi, L. (2023). Simulating heat and CO<sub>2</sub> fluxes in Beijing using SUEWS V2020b: Sensitivity to vegetation phenology and maximum conductance. *Geosci. Model Dev.*, 16(15):4551–4579, DOI: 10.5194/gmd-16-4551-2023
- IV** **Havu, M.**, Kulmala, L., Lee, H.S., Saranko, O., Soininen, J., Ahongshangbam, J., and Järvi, L. (2023). CO<sub>2</sub> uptake of urban vegetation in a warming Nordic city. *Urban For. Urban Green.* (in review)

# 1 Introduction

The anthropogenic greenhouse gas emissions have increased steadily over the recent decades, posing a pressing need for immediate reductions to limit global warming to 2°C by 2100 (Canadell et al., 2021). Simultaneously, urbanization is a global trend, with over 55% of the world’s population residing in cities, with projections indicating for it to increase to 68% by mid-century (UN, 2019). Urban areas currently contribute to 67–72% of global emissions (Lwasa et al., 2022), and the ongoing urbanization trend is set to amplify this contribution, emphasizing the vital role of cities in achieving carbon neutrality goals. An increasing number of cities are establishing their own climate targets, with varying levels of ambition in comparison to national goals (Salvia et al., 2021). To attain these targets, cities must concurrently transition towards more sustainable production methods, adopt low-carbon energy sources, electrify their infrastructure, and enhance carbon uptake and storage within urban green areas (Lwasa et al., 2022). While the contribution of urban green has often been overlooked, recent studies have increasingly highlighted the importance of vegetation and soil in the urban carbon cycle as they offset part of the emissions (Weissert et al., 2014). In addition, urban vegetation offers other co-benefits such as cooling (Rahman et al., 2020; Winbourne et al., 2020), improved water management (Berland et al., 2017), and enhanced well-being (Wolf et al., 2020). On the contrary, street trees have the potential to diminish air quality within street canyons by hindering pollutant dispersion (Karttunen et al., 2020).

Assessing the carbon uptake of urban vegetation is also critical for urban observational networks (Christen, 2014). Numerous observation methods to estimate cities’ emissions have been explored globally, such as eddy covariance (EC) measurements (e.g. Crawford et al., 2011; Järvi et al., 2012; Ward et al., 2015), tall-tower inversion systems (Lian et al., 2023), and remote sensing (Kiel et al., 2021; Schuh et al., 2021; Dietrich et al., 2021), while several ongoing projects aim to develop a comprehensive method for measuring emissions in cities (Mitchell et al., 2022; Christen et al., 2023). However, these measurement methods typically capture the net exchange of carbon dioxide (CO<sub>2</sub>), including both anthropogenic and biogenic sources and sinks. This introduces uncertainties of unknown magnitude into the estimation of anthropogenic emissions. To distinguish between CO<sub>2</sub> components, each having their own diurnal and seasonal cycles, requires methods that assess CO<sub>2</sub> exchanges from urban vegetation and soil with high temporal resolution. Progress has been made in measurement techniques,

for instance using carbonyl sulfide (COS) as a proxy for estimating biogenic sinks (Karl et al., 2020), as well as using radiocarbon measurements to distinguish between anthropogenic and biogenic sources (Weissert et al., 2016b). Nevertheless, as these empirical methods have varying source areas, further refinement is required to reduce uncertainties, underscoring the need for modelling tools for partitioning different CO<sub>2</sub> components in the net exchange.

The biogenic sources and sinks can be further divided into CO<sub>2</sub> uptake by photosynthesis, along with plant and soil respiration. Commonly, assessments of carbon sinks and stocks in urban green primarily focus on above-ground vegetation, overlooking the substantial carbon reservoirs within the soil. The CO<sub>2</sub> exchange components exhibit significant variability based on meteorological conditions such as air temperature, radiation, and humidity, as well as environmental conditions like soil moisture and temperature. In contrast to a natural ecosystem, CO<sub>2</sub> exchange in urban areas can be influenced by factors such as elevated local temperatures resulting from the urban heat island effect (Oke, 1982), soil water availability impacted by excess runoff or additional water inputs from irrigation (Nielsen et al., 2007), and various management practices such as mowing (Velasco et al., 2021) or fertilization (Livesley et al., 2010).

Models that simulate different components of biogenic CO<sub>2</sub> exchange complement measurement methods and enable high-resolution quantification of CO<sub>2</sub> cycles across entire cities. Models are particularly valuable when measurements are not available or when future projections are required. These models rely on accurate measurements for calibration and have been explored in urban areas using various approaches, including tree biomass growth models such as i-Tree (Nowak and Crane, 2000), satellite-based models e.g. VPRM (Hardiman et al., 2017; Wang et al., 2021; Wei et al., 2022; Lian et al., 2023) and diFUME (Stagakis et al., 2023b), as well as urban land surface models (e.g. SURFEX, Goret et al., 2019). i-Tree, widely used for assessing carbon sequestration by trees to support urban climate initiatives, heavily relies on measurements and climate data from the US. It provides only annual estimates and does not account for soil contributions. While satellite-based models are proficient at capturing vegetation phenology, they may face challenges when translating vegetative indices into the underlying physiological processes like photosynthesis and respiration. Thus, these models need to be calibrated either using EC observations from regions with similar climate as the city (e.g., VPRM) or by using urban EC observations (e.g., diFUME). However, these models are not suitable for projecting future conditions as they rely on

satellite measurements. On the other hand, urban land surface models require calibration to estimate vegetation phenology. Still, they possess the advantage of being able to integrate the physiological processes and stresses experienced by urban vegetation. Furthermore, they can be adjusted to account for future climate scenarios.

This thesis aims to advance our understanding of urban CO<sub>2</sub> exchange across various scales, from street tree plantings to neighbourhood and city levels (see Fig. 1). As part of the thesis, the CO<sub>2</sub> module is implemented within the urban land surface model SUEWS (Surface Urban Energy and Water Balance Scheme, Järvi et al., 2011; Ward et al., 2016), allowing integrated research with urban water and energy balances. The following main research questions will be addressed:

**1. Is the urban land surface model SUEWS applicable to simulate urban CO<sub>2</sub> exchange?**

The research incorporates CO<sub>2</sub> exchange into the urban land surface model SUEWS (**Paper I**) and assesses its performance against EC measurements conducted in Helsinki (**Paper I**) and Beijing (**Paper III**), as well as against street tree measurements in Helsinki (**Paper II**).

**2. What is the role of soil in CO<sub>2</sub> exchange of newly planted street trees?**

In **Paper II**, the developed CO<sub>2</sub> module in SUEWS and the soil carbon model Yasso are utilized to examine the role of soils on urban CO<sub>2</sub> exchange of street tree plantings over the following 30 years after the street construction.

**3. How does biogenic CO<sub>2</sub> exchange vary with different surface covers in Helsinki, and how will this be changed by climate change?**

**Paper IV** employs the SUEWS model across the entirety of Helsinki, categorizing CO<sub>2</sub> exchange based on local climate zones (LCZs). The results simulated with the current climate (2015–2019) are compared against conditions in the 2050s using the RCP8.5 scenario.

**4. To what extent can biogenic CO<sub>2</sub> exchange offset anthropogenic emissions in different scales?**

**Papers I** and **III** examine the role of biogenic CO<sub>2</sub> exchange in comparison to anthropogenic emissions at neighbourhood scale (i.e the scale of eddy covariance measurements), while **Paper IV** focuses on estimating the city-level offset.

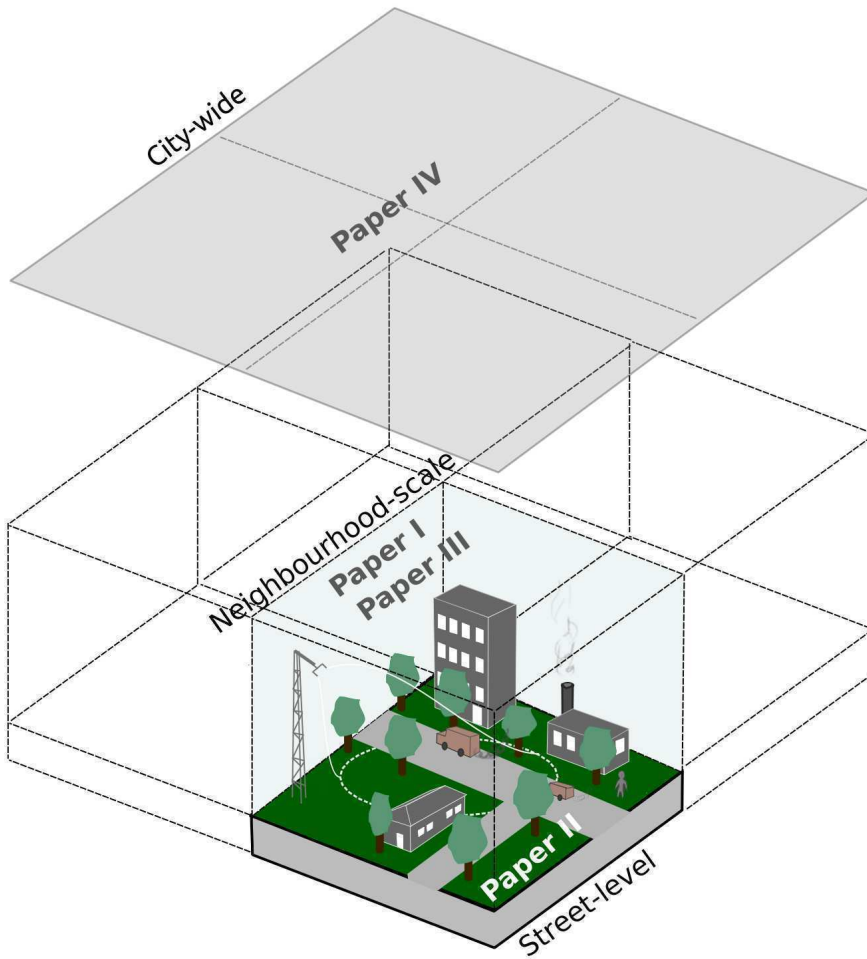


Figure 1: Schematic illustration of the different scopes of the papers included in this thesis.

## 2 Surface-atmosphere interactions

### 2.1 Urban boundary layer

The lowest part of the atmosphere is referred to as atmospheric boundary layer (BL), where turbulent processes dominate the air flow (Stull, 1988). In urban areas, an internal boundary layer known as the urban boundary layer (UBL) develops due to the presence of buildings, roads, and other infrastructure that disrupt the natural airflow and alter the local climate (Oke et al., 2017). Figure 2 depicts the structure of the UBL and its different sublayers. This alteration in the urban environment leads to notable changes, including variations in turbulence intensity, significant shifts in the urban water balance, and the development of the urban heat island effect (UHI, Oke, 1982). The magnitudes of these changes can vary considerably within urban areas.

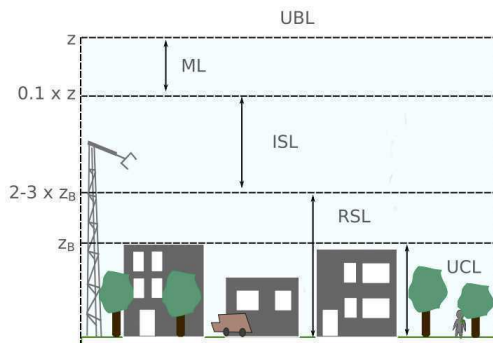


Figure 2: Schematic illustration of simplified urban boundary layer (UBL) divided into urban canopy layer (UCL), roughness sublayer (RSL), inertial sublayer (ISL), and mixed layer (ML). (Modified after Oke et al., 2017.)

The urban environment significantly alters the water balance compared to natural ecosystems (Grimmond et al., 1986). Urban landscapes consist of various surface cover types, with impervious surfaces sealing the soil beneath, limiting soil-atmosphere interactions. Irrigation is commonly used to sustain vegetation, while impervious surfaces contribute to increased surface runoff (Kokkonen et al., 2018). In addition, urban vegetation, or its lack, plays a crucial role in surface-atmosphere interactions by con-

tributing to the exchange of water vapour (Grimmond and Oke, 1991), and CO<sub>2</sub>.

A prominent phenomenon observed within the UBL is the urban heat island effect (UHI, Oke, 1982). UHI results from the influence of built surfaces and human activities, which lead to elevated temperatures within cities, surpassing those observed in corresponding rural regions. Particularly, UHI is influenced by a range of factors, including reduced vegetation, alterations in radiation patterns caused by shading and variations in surface albedo, as well as heat emissions originating from transportation, energy consumption, and humans. UHI can be categorized into various scales (Oke et al., 2017), with the canopy layer heat island (UHI<sub>UCL</sub>) being the most significant concerning its impact on turbulent exchanges. UHI<sub>UCL</sub> involves differences between temperatures within the urban canopy layer (UCL, Fig. 2) compared to corresponding heights in rural locations. Research on UHI<sub>UCL</sub> has mostly relied on traditional air temperature measurements or modelling approaches (Mirzaei and Haghighat, 2010; Mirzaei, 2015; **Paper IV**). In European cities, UHI has been documented to exhibit significant variability (Santamouris, 2007). Estimates of UHI intensity span a wide range, from 1.6°C in Vienna, Austria (Böhm, 1998), to as high as 12°C in Lodz, Poland (Klysik and Fortuniak, 1999).

UHI strongly depends on the surface cover and human activities which can be described using Local Climate Zone (LCZ, Stewart and Oke, 2012) classification. LCZ categorizes cities and their neighbourhoods into different classes based on their built and land cover characteristics. Originally designed to help understand urban heat studies, LCZ research has grown to include a wide range of application (Huang et al., 2023). In addition to studying UHI (Stewart et al., 2014; Bechtel et al., 2019) and thermal comfort (Aminipouri et al., 2019), LCZs have been used in various spatial analyses, including urban meteorology (Tse et al., 2018), air pollution (Shi et al., 2019), anthropogenic heat (Rathnayake et al., 2020), and CO<sub>2</sub> emission (Wu et al., 2018; Mouzourides et al., 2019) studies. Moreover, the heat-related risk between LCZs has been studied using different Representative Concentration Pathway (RCP) scenarios and urban planning strategies (Verdonck et al., 2019; Aminipouri et al., 2019; Gál et al., 2021). In this thesis, **Paper IV** extends LCZ analysis to include the assessment of biogenic CO<sub>2</sub> exchange components.

## 2.2 Urban net CO<sub>2</sub> exchange

The CO<sub>2</sub> exchange between natural ecosystems and the atmosphere includes physiological processes such as plant photosynthesis ( $F_{pho}$ ), and plant and soil respiration ( $F_{res}$ ). Beyond biogenic CO<sub>2</sub> exchange, urban areas are a great source of CO<sub>2</sub> due to anthropogenic activities (Fig. 3). Anthropogenic CO<sub>2</sub> ( $F_{C,ant}$ ) is locally emitted from combustion of varying sources such as vehicles and building heating, and from the respiration of humans and animals. This balance for the urban net CO<sub>2</sub> exchange ( $F_C$ ) can be expressed as (adobted from Christen, 2014):

$$F_C = F_{C,ant} + F_{pho} + F_{res}. \quad (1)$$

In this thesis, the main focus is on the biogenic components  $F_{pho}$  and  $F_{res}$ .

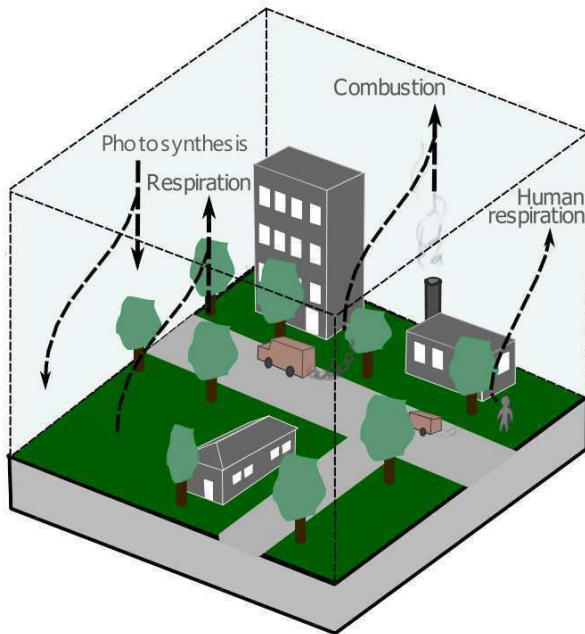


Figure 3: Schematic illustration of simplified urban CO<sub>2</sub> exchange components. (Modified after Christen, 2014.)

Photosynthesis is the biological process in which vascular plants assimilate atmospheric CO<sub>2</sub> through small leaf openings known as stomata, and produce carbohydrates within their chlorophyll-containing tissues (Hari and Kulmala, 2008). The rate of CO<sub>2</sub> uptake by photosynthesis depends on various factors, including light, water availability, as well as air temperature, humidity, and the concentration of CO<sub>2</sub> in the air.

Light is a fundamental requirement for photosynthesis. As the intensity of photosynthetically active radiation (PAR) increases, photosynthesis rates also rise, although this response eventually saturates. Furthermore, hydrologic stress in plants influences photosynthesis. This stress results from the connection between photosynthesis and transpiration processes, both of which occur simultaneously but in opposite directions through stomatal openings. When plants need to conserve water, they frequently respond by closing their stomata, which consequently restricts the process of photosynthesis. Hydrologic stress is determined by the combined influence of soil moisture supply and atmospheric water demand (Novick et al., 2016). Soil moisture is generally sufficient until the point where soil water content approaches the permanent wilting point, beyond which photosynthesis capability is severely diminished (Reich et al., 2018). Additionally, dry air conditions, particularly when vapour pressure deficit (VPD) is high, contribute to hydrologic stress. Under such conditions, increased transpiration occurs, but to conserve water, plants tend to close their stomata. The air humidity can also be expressed with specific humidity deficit (Ogink-Hendriks, 1995). Photosynthesis is also temperature dependant, as elevated temperatures generally lead to increased photosynthesis rates, but excessively high temperatures can cause damage and reduce the efficiency of photosynthesis (Sage et al., 2008; Niu et al., 2012; Chang et al., 2021; Kunert et al., 2022). The optimal temperature for photosynthesis is typically associated with leaf temperature, and the optimal temperature usually falls within the range of 20 to 35°C (Sage et al., 2008). However, the optimal temperature range can shift. For instance, higher CO<sub>2</sub> concentrations (Sage et al., 2008) or elevated growth temperatures (Hikosaka et al., 2006), can both influence the optimum temperature range, potentially leading to an increase in optimal temperature. In addition, elevated concentration of CO<sub>2</sub> in the atmosphere can result in higher photosynthesis rates (Nowak et al., 2004; Taylor et al., 2008).

Organisms break down carbohydrates and other organic carbon compounds to acquire energy for their vital processes and growth. This process releases CO<sub>2</sub>, which can be further divided into autotrophic or heterotrophic respiration (Hari and Kulmala, 2008).

Autotrophic respiration refers to the process of respiration carried out by vegetation, whereas heterotrophic respiration refers to the metabolism of other species. Here, it mainly refers to the decomposition of organic matter by microorganisms. The rate of CO<sub>2</sub> resulting from autotrophic respiration depends on plant biomass and activity. Usually, the plant activity increases with increasing temperature and hence autotrophic respiration is often estimated as a function of biomass and temperature (Ryan et al., 1997; Gibelin et al., 2008; Launiainen et al., 2015; Stagakis et al., 2023b). Heterotrophic respiration in soil depends on the physical conditions (soil temperature and moisture), and the amount and quality of organic carbon (Ise and Moorcroft, 2006).

Photosynthesis per leaf area is expected to be higher in urban environments compared to natural ecosystems (Hardiman et al., 2017), due to elevated temperatures caused by UHI. This phenomenon extends the growing season and subsequently enhances the rate of photosynthesis (Melaas et al., 2016; Briber et al., 2015; Zhao et al., 2016). On the other hand, excessively high temperatures can cause stomatal closure, reducing photosynthesis rates (Wang et al., 2021). In addition, urban areas often benefit from irrigation, which helps alleviate water stress (Nielsen et al., 2007). Urban areas may also experience higher soil respiration rates due to management practices such as fertilization or the use of mulch around plants (Decina et al., 2016). Moreover, the elevated temperatures caused by UHI can lead to higher respiration rates (Wang et al., 2021). In contrast, photosynthesis and respiration per land area tend to be lower in urban areas due to the greater proportion of impervious surfaces (Nordbo et al., 2012a; Briber et al., 2015; Ward et al., 2015; **Paper IV**). The rising temperatures associated with climate change can also impact UHI and local environmental conditions, consequently influencing both photosynthesis and respiration processes (Wang et al., 2021; **Paper IV**).

## 2.3 Empirical quantification of CO<sub>2</sub> and water exchanges

Biogenic net CO<sub>2</sub> exchange can be assessed across various urban scales through the application of diverse measurement techniques. Each of these methods comes with its unique set of challenges and advantages. Some measurements capture signals from both biogenic and anthropogenic sources over a large area (e.g. eddy covariance, **Papers I and III**), while others focus on specific aspects of the urban environment (e.g. chamber measurements, **Papers II and IV**), necessitating scaling for broader applica-

tion. Additionally, heterotrophic respiration rates can be indirectly assessed through low-frequency carbon storage measurements. Besides measurements of actual CO<sub>2</sub> exchange, transpiration measurements such as sap flow (**Paper II**) can provide valuable insights into vegetation behaviour and stomatal opening.

Measurements have a vital role in calibrating models to align with the complexities of urban dynamics (Grimmond, 2006; Decina et al., 2016; **Paper I–III**; Stagakis et al., 2023b). Furthermore, models serve as valuable tools for extending measurements obtained at the plot level to provide city-wide estimates (Decina et al., 2016; **Paper IV**). They also play a crucial role in making projections related to future climate scenarios (Wang et al., 2021; **Paper IV**).

The following measurement techniques utilized in this thesis are instrumental in the calibration and evaluation of biogenic CO<sub>2</sub> models employed in urban areas:

**Eddy covariance technique (EC)** is a widely adopted technique for quantifying the vertical exchange of CO<sub>2</sub> (or any mass, energy, and momentum) between the Earth’s surface and the atmosphere (Aubinet et al., 2012). To accurately capture the vertical exchange or transport caused also by the smallest eddies, EC measurements require a high measurement frequency, typically 10 Hz. For EC measurements, an ultrasonic anemometer and an infrared gas analyzer (IRGA) are employed. The ultrasonic anemometer measures the three wind components ( $u$ ,  $v$ ,  $w$ ) and sonic temperature, determining the time it takes for an ultrasonic pulse to travel between sensors with known distances, dependent on the speed of sound and air velocity along the path. The IRGA measures gas concentrations, such as CO<sub>2</sub> and water vapor (H<sub>2</sub>O) mole fractions, detecting light absorption within an absorption band.

EC measurements should be made at a considerable height within the boundary layer, ensuring they fall within the inertial sublayer (ISL), where turbulence can be assumed to be constant with height and horizontally homogeneous. In practice, the height of the roughness sublayer (RSL) can be substantial in urban areas, sometimes resulting in measurements being located within the RSL. However, it has been observed that the flux-gradient relationship effectively models turbulent exchanges near the upper boundary of the RSL (Vogt et al., 2006). Although making measurements within the RSL might be unavoidable, it introduces additional uncertainties into the EC method.

EC measurements represent a certain surface area upwind of the EC measurement point called source area or footprint (Kljun et al., 2004; Aubinet et al., 2012). The

footprint of EC measurements relies on various factors, including the measurement height, topography, wind speed, and atmospheric stability. In urban areas, commonly used analytical footprint models do not adequately consider the complexity of the urban surface (Vesala et al., 2008). Thus, observations are often examined based on different wind sectors (Järvi et al., 2012; Karsisto et al., 2016; **Papers I, III**). EC measurements capture signals from both biogenic and anthropogenic sources across a wide spatial extent and are unable to distinguish between them. Although EC measurements are the most direct mean to measure the net CO<sub>2</sub> exchange between the surface and the atmosphere, they encounter several challenges that necessitate post-processing (Sabbatini et al., 2018). For instance, under stable nighttime conditions, horizontal advection and storage effects can introduce complexities to the representativeness of the measurements. Given the diverse conditions under which EC measurements may encounter limitations, it becomes crucial to filter data to remove unrepresentative observations. These data gaps can be substantial, and if annual estimations of fluxes are required, appropriate gap-filling methods must be employed to ensure comprehensive coverage (Menzer et al., 2015).

**Chamber measurements** serve as a valuable tool for studying gas fluxes arising from soil and vegetation interactions with the atmosphere by enclosing specific plant parts (**Papers II and IV**) or soils areas (Järvi et al., 2012; Weissert et al., 2016a; **Paper IV**) within a chamber (Livingston and Hutchinson, 1995). These measurements focus on quantifying the responses of gas fluxes in these specific parts to changing environmental conditions by analysing changes in gas concentration over time within the chamber. Chamber measurements can be classified into two main categories: closed and open systems. Closed systems estimate gas fluxes by observing the temporal change in gas concentration within the sealed chamber, while open systems calculate fluxes by comparing gas concentrations between the inflowing and outflowing air. These chambers can be operated either manually or automatically. Moreover, the chambers can be categorized based on their transparency or coverage. Transparent chambers are utilized when studying photosynthesis, as they allow light to penetrate the chamber and the light response of photosynthesis can be determined by repeating the measurements in different light intensities. On the other hand, covered chambers, referred to as dark chambers, serve to investigate respiration by blocking light. Within the chamber, the gas fluxes are quantified using a gas analyzer, coupled with sensors for measuring radiation, temperature, and humidity.

Chamber measurements provide valuable insights into the relationship between component fluxes and environmental factors in urban green areas (Vesala et al., 2008; Järvi et al., 2012; Weissert et al., 2016a; Decina et al., 2016; **Paper II**). Nevertheless, chamber measurements have their own limitations. The chamber is not always airtight, manual measurements provide only momentary data so multiple repetitions are required, and the measurements could potentially disrupt the measured vegetation. Moreover, when scaling up these chamber measurements to represent larger areas or ecosystems, it becomes necessary to employ models that consider various environmental factors and microclimatic conditions.

**Carbon stock measurements** are one method for assessing net exchange by tracking alterations in carbon storage throughout the study period. This method can provide insights into urban carbon stock variations on an annual or less frequent basis (Riikonen et al., 2017; **Paper II**). These measurements encompass the estimation of both vegetation carbon and soil carbon stocks. Vegetation carbon estimation relies on quantifying biomass, tracking changes therein, and estimating the carbon content within it. Soil carbon, often described as soil organic carbon (SOC) stocks, is determined through soil sampling. Quantification is typically achieved using the loss-on-ignition (LOI) method, which involves the removal of organic matter through heat application and then assessing the resulting mass alteration. Subsequently, an assumption is made regarding the proportion of carbon within the LOI. The method is limited by the necessity for long-term monitoring of stock changes, especially in the context of soil where alterations occur gradually. Consequently, the approach is demanding in terms of labor, and time-consuming.

**Sap flow** sensors are instruments designed to quantify transpiration flow (**Paper II**) by monitoring the upward movement of sap within xylem tissue (Granier, 1987). These sensors can be strategically deployed in different regions of the tree, such as stems, trunks, branches, or tillers. The process of sap flow is influenced by the regulation of stomatal opening.

Various techniques are available for measuring sap flow, but they all share a common principle: the utilization of heat as a tracer (Hölttä et al., 2015; Flo et al., 2019; Poyatos et al., 2020). In one approach, specific sections of the plant are heated, and the subsequent measurement involves tracking heat loss and dissipation. Alternatively, a heat pulse is generated and sent through the plant, with the flow rate calculated based on the time required for this heat pulse to traverse a specific distance. Using sap flow

measurements to estimate transpiration has inherent limitations. These measurements often lag behind canopy transpiration (Schulze et al., 1985), and to scale these measurements to estimate whole-plant sap flow rates, it is essential to have at least an estimate of the sapwood area (Poyatos et al., 2020).

## 3 Materials and methods

### 3.1 Sites and measurements

In **Papers I** and **II**, the model evaluation and examination of CO<sub>2</sub> exchanges took place at three distinct locations within Helsinki, Finland: the suburban site Kumpula (**I**), the city centre Tornio (**I**), and the street tree site Viikki (**II**). The evaluation extended to Beijing, China, in **Paper III**. Lastly, **Paper IV** entailed city-wide application within Helsinki to calculate CO<sub>2</sub> exchanges and their dependency on land cover.

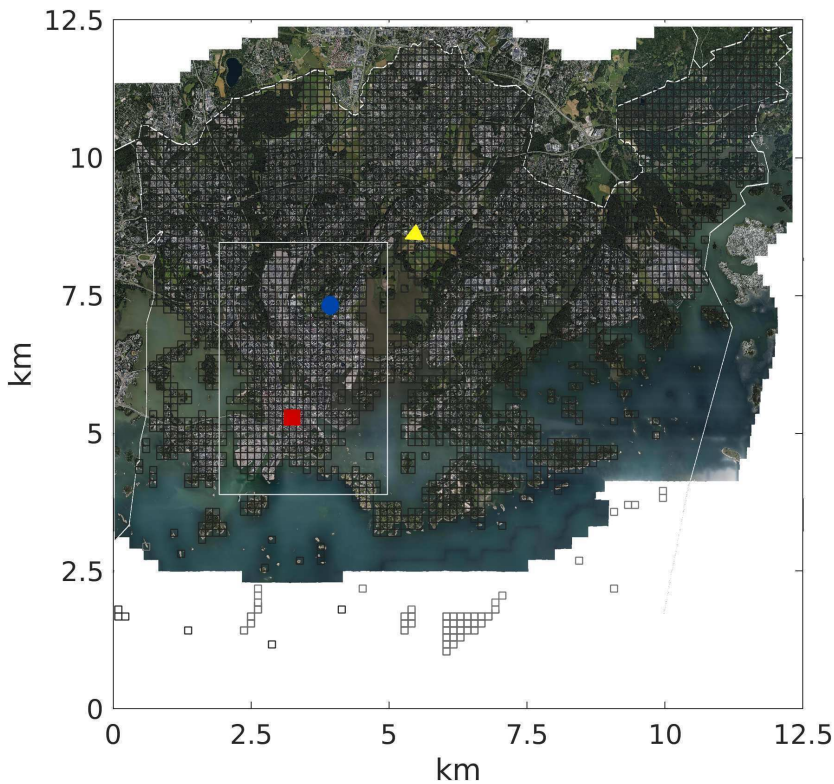


Figure 4: Aerial photo of Helsinki (©Kaupunkimittausosasto, 2017) with the three study sites: Kumpula (blue circle, **I**), Tornio (red square, **I**), and Viikki (yellow triangle, **II**). The city is divided into 250 x 250 m<sup>2</sup> grids used in **Paper IV** and the rectangular white box indicating the area used in **Paper I**.

### 3.1.1 Helsinki

Helsinki, the capital of Finland ( $60^{\circ}10'N$ ,  $24^{\circ}56'E$ , Fig. 4), is situated along the coast of the Baltic Sea. The climate of Helsinki falls under the classification of humid continental with warm summers (Dfb), with the mean annual temperature of  $6.5^{\circ}C$  and an annual precipitation of 656 mm (Jokinen et al., 2021). The temperatures in Helsinki are projected to be  $2^{\circ}C$  warmer, with approximately 70 mm more precipitation due to climate change in the 2050s (Saranko et al., 2020; **Paper IV**). The total land area of the city spans  $214.19 \text{ km}^2$ . In **Papers I** and **IV**, the city centre and further the whole city were divided into  $250 \times 250 \text{ m}^2$  size grids (Fig. 4).

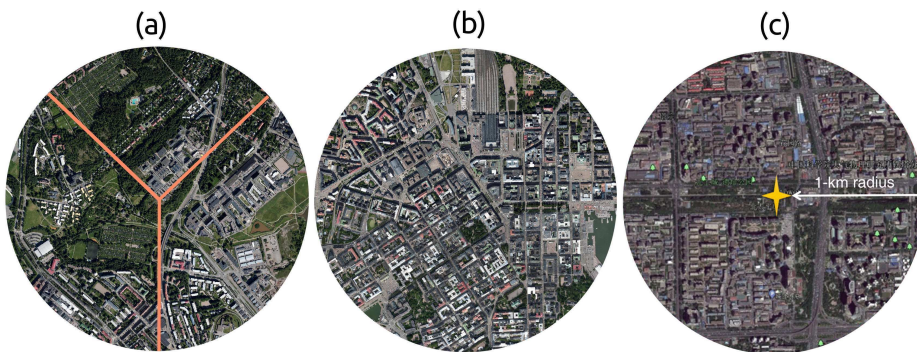


Figure 5: Aerial photos of the study areas with 1-km radius around (a) Kumpula with its three sectors (©Kaupunkimittausosasto, 2017), (b) Tornio (©Kaupunkimittausosasto, 2017), and (c) Beijing EC stations (Google Earth, image ©2022 Maxar Technologies).

#### **Kumpula suburban site**

The SMEAR III station (*Station of Measuring Ecosystem-Atmosphere Relationships*) is situated in the semiurban area of Kumpula, located 4 km northeast of the city centre ( $LCZ = 6$ ) (Järvi et al., 2009; **Paper I**). Within a radius of 1 km surrounding the 31-m measurement mast (Fig. 5a), approximately half of the area is covered by vegetation. The northern region of the tower ( $320-40^{\circ}$ , referred to as Ku1) encompasses the university campus, while further away, there are suburban low-height apartment buildings with small gardens. Moving eastward ( $40-180^{\circ}$ , Ku2), emissions originate from one of the main roads leading to the Helsinki city centre. The zone between

the road and the mast is covered by a broadleaf forest. Towards the southwest (180–320°, Ku3), there are parks, the University Botanical Garden, and allotment gardens, vegetation covering 59% of the sector. In this direction, the nearest road is situated 800 m away from the measurement mast. EC measurements were initiated in 2005 and are ongoing (Vesala et al., 2008).

### **Torni city centre site**

The measurement site Torni is situated in the highly built-up city centre (LCZ = 2) (Nordbo et al., 2013; Karsisto et al., 2016; **Paper I**). Within a 1-km radius circle surrounding the site (Fig. 5b), the average building height reaches 18 m, while the proportion of vegetated cover is 20%, comprising mainly street trees and a few parks. The measurement station is situated atop Hotel Torni, at an elevation of 60 m. The EC measurements were established in 2010 and continue to be operational (Nordbo et al., 2012b).

### **Viikki street tree site**

The street tree study site is located in Viikki, Helsinki (N60°15', E25°03'), approximately 9 km northeast of the Helsinki city centre (**Paper II**). Two streets were intensively studied from 2002 to 2016, focusing on either *Tilia x vulgaris* Hayne or *Alnus glutinosa* (L.) Gaertn. f. *pyramidalis* 'Sakari' tree species (Riikonen et al., 2011, 2016, 2017). Three different soil types were studied at both streets. Soil 1 primarily consisted of sand, clay, and peat; Soil 2 comprised composted sewage sludge mixed with sand, pine bark, and peat; and Soil 3 was a blend of fine gravel, sand, clay, leaf compost, and pine bark. Throughout the study period, comprehensive monitoring of tree characteristics, gas exchange processes, sap flow, and soil carbon content was conducted. The street with *Tilia* trees corresponds to LCZ 9 and the one with *Alnus* trees to LCZ 6. For the purpose of this study, the combined entities of trees and their underlying growing media (i.e., soil) are collectively referred to as street tree plantings.

### **3.1.2 Beijing**

Beijing, the capital of China, exhibits a monsoon-driven continental climate (Dwa), with the mean annual temperature of 12.5°C and an annual precipitation of 592 mm (Liu et al., 2023). The EC measurement setup (Fig. 5c) is positioned at an elevation of 47 m on the Institute of Atmospheric Physics (IAP) meteorological tower (N39°58', E116°22') (Liu et al., 2012; **Paper III**). This tower is 325 m tall and is located in

the northwest region of Beijing. The immediate vicinity of the tower is primarily characterized by impervious surfaces, constituting about two-thirds of the surrounding area, while the remaining portions (29%) are covered with vegetation. The site aligns with LCZs 1 and 2, featuring an average building height of 19.1 m. There is significant vehicular traffic in the vicinity, particularly to the east and north of the tower. The flux measurements commenced in 2012.

## 3.2 CO<sub>2</sub> modelling

The thesis focuses on the development (**Paper I**), evaluation (**Papers I, II, III**), and application (**Papers I–IV**) of the CO<sub>2</sub> module within the urban land surface model SUEWS. Moreover, the investigation into the dynamics of soil carbon decomposition in urban soils is extended through the application of the Yasso model in **Paper II**.

### 3.2.1 SUEWS

#### Model description

The Surface Urban Energy and Water Balance Scheme (SUEWS) is an urban land surface model originally designed to operate at the neighbourhood-scale, simulating the energy and water balances of urban surfaces (Järvi et al., 2011; Ward et al., 2016). Within the SUEWS model, several submodels are incorporated to account for diverse factors, including net all-wave radiation (Offerle et al., 2003), storage processes (Grimmond and Oke, 1991; Sun et al., 2017), anthropogenic heat fluxes, snow, and irrigation (Järvi et al., 2014). In addition, it can simulate the local 2 m air temperature and relative humidity in the roughness sublayer (Tang et al., 2021).

SUEWS distinguishes between seven surface types: paved surfaces, buildings, evergreen trees and shrubs, deciduous trees and shrubs, grass, bare soil, and water. To effectively model each of these surface types, specific input parameters are necessitated. These include details such as plan area fractions, albedo, emissivity, moisture storage capacity, building height, and tree height. Moreover, the model is driven by various meteorological variables, including wind speed, relative humidity, air temperature, air pressure, precipitation, and short-wave radiation. These meteorological inputs are fundamental in shaping the model’s performance and outcomes.

In **Paper I**, a new CO<sub>2</sub> module was introduced to the SUEWS model to compute the total CO<sub>2</sub> exchange ( $F_C$ ,  $\mu\text{mol m}^{-2}\text{s}^{-1}$ ), while accounting for both local-scale anthropogenic emissions ( $F_{C,ant}$ ) and biogenic components ( $F_{C,bio}$ ) of CO<sub>2</sub> exchange. The anthropogenic components include CO<sub>2</sub> emissions from human metabolism ( $F_M$ ), vehicles ( $F_V$ ), building energy and heating/cooling combustion (involving natural gas, coal, and wood) ( $F_B$ ), and local-scale point sources ( $F_P$ ). The biogenic components encompass CO<sub>2</sub> uptake by photosynthesis ( $F_{pho}$ ) and release through respiration ( $F_{res}$ ).

The net exchange is as follows:

$$F_C = F_{C,ant} + F_{C,bio} = F_M + F_V + F_B + F_P + F_{pho} + F_{res}, \quad (2)$$

where positive values denote CO<sub>2</sub> sources and negative values indicate CO<sub>2</sub> sinks with respect to the atmosphere.

The simulation of biogenic CO<sub>2</sub> components  $F_{pho}$  and  $F_{res}$  is based on their connection to meteorological conditions. The estimation of  $F_{pho}$  is based on how sensitive the stomatal opening is to the different environmental factors that control it. The estimation of  $F_{pho}$  connects it to the surface resistance, or its inverse, the surface conductance that is required to model the latent heat flux ( $Q_E$ ), using the Penman-Monteith equation (Penman, 1948; Monteith, 1965) modified for urban environments (Grimmond and Oke, 1991). The surface conductance ( $g_s$ , mm s<sup>-1</sup>) is estimated with modified Jarvis-Stewart formulation (Jarvis, 1976; Stewart, 1988):

$$g_s = G_1 \sum_i (f r_i g_{i,max} \frac{LAI_{d,i}}{LAI_{m,i}}) g_K g_q g_T g_\theta, \quad (3)$$

where  $g_s$  is calculated separately for each vegetation type  $i$  (evergreen, deciduous, or grass) and then summed together. Parameter  $G_1$  (mm s<sup>-1</sup>) is connecting the leaf level opening to canopy level,  $f r_i$  is the fraction of each vegetation cover,  $g_{i,max}$  (mm s<sup>-1</sup>) is the maximum conductance,  $LAI_{d,i}$  (m<sup>2</sup> m<sup>-2</sup>) is the daily leaf area index, which is divided with the maximum value of LAI ( $LAI_{m,i}$ ). The four g-functions are the environmental response functions  $g_K$ ,  $g_q$ ,  $g_T$ , and  $g_\theta$  on shortwave radiation, specific humidity deficit, air temperature, and soil moisture deficit, respectively. These functions vary between 0 and 1. The same environmental response functions are now included into the  $F_{pho}$  (μmol m<sup>-2</sup>s<sup>-1</sup>) simulation, where the maximum photosynthesis per leaf area  $F_{pho,max,i}$  (μmol m<sup>-2</sup>s<sup>-1</sup> LAI<sup>-1</sup>) for each vegetation type  $i$  obtained from measurements, is scaled with these response functions together with the simulated  $LAI_{d,i}$  (**Paper I**):

$$F_{pho} = \sum_i (f r_i F_{pho,max,i} LAI_{d,i}) g_K g_q g_T g_\theta. \quad (4)$$

Here, the g-functions use slightly different notations compared to **Papers I–IV**. The functions have the following forms (Fig. 6, Ward et al., 2016). The function form relating to shortwave radiation follows Stewart (1988):

$$g_K = \frac{K_\downarrow / (G_2 + K_\downarrow)}{K_{\downarrow,max} / (G_2 + K_{\downarrow,max})}, \quad (5)$$

where  $K_{\downarrow, max}$  is the maximum shortwave radiation.

The function for specific humidity deficit can be described with linear (Jarvis, 1976; Stewart, 1988) or nonlinear response to increasing deficit (Ogink-Hendriks, 1995). Following Ward et al. (2016), the nonlinear responses are used for specific humidity response:

$$g_q = G_3 + (1 - G_3)G_4^{\Delta q}, \quad (6)$$

The function for air temperature is based on optimal temperatures for photosynthesis ( $T_{air} = G_5$ ) by Stewart (1988):

$$g_T = \frac{(T_{air} - T_L)(T_H - T_{air})^{T_C}}{(G_5 - T_L)(T_H - G_5)^{T_C}}, \quad (7)$$

where  $T_L$  and  $T_H$  are the lowest and highest hourly air temperatures where stomata can be open, and where

$$T_C = \frac{(T_H - G_5)}{(G_5 - T_L)}. \quad (8)$$

The function for soil moisture ( $\theta$ ) depends on when the wilting point (WP) is reached and no more water is available for plants (Ward et al., 2015; Stewart, 1988):

$$g_\theta = \frac{1 - \exp(G_6(\Delta\theta - \Delta\theta_{WP}))}{1 - \exp(-G_6\Delta\theta_{WP})}. \quad (9)$$

The simulation of  $F_{res}$  ( $\mu\text{mol m}^{-2}\text{s}^{-1}$ ) is based on its exponential relation to air temperature:

$$F_{res} = \sum_i fr_i \max(a_i \cdot \exp(T_{air}b_i), 0.6), \quad (10)$$

where the rate of respiration is simulated with empirical constants  $a$  and  $b$ , which represent the flux rate at  $0^\circ\text{C}$  and the temperature sensitivity, respectively. The function is given a minimum value of  $0.6 \mu\text{mol m}^{-2}\text{s}^{-1}$ , based on wintertime respiration rates (Pumpanen et al., 2015).

### Biogenic model parameterization

The parameters for equations (3)–(10) can be obtained from existing literature or determined through measurements (Järvi et al., 2011; Ward et al., 2016; **Papers I–IV**). These equations are fitted against either measured photosynthesis or respiration using the least-squares fitting approach, involving the random selection of seven-eighths

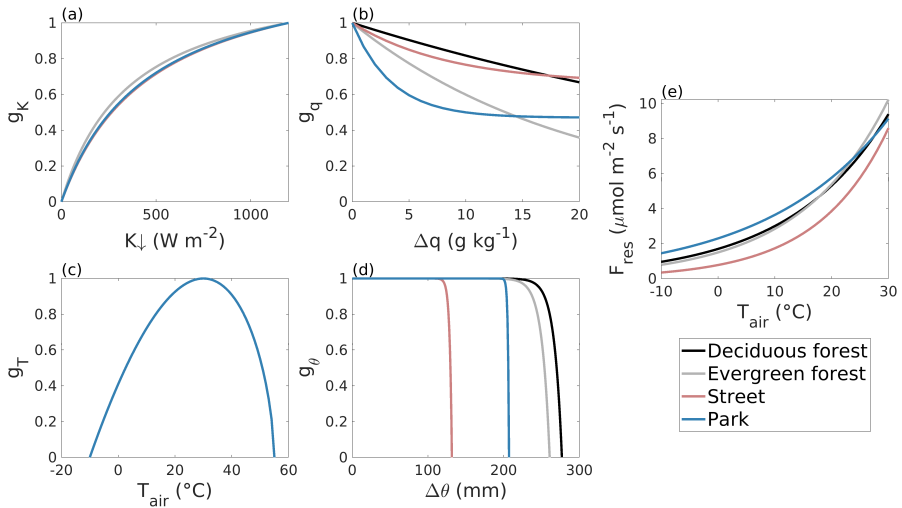


Figure 6: Examples of surface conductance dependencies on environmental factors as presented in **Paper IV**: (a) shortwave radiation ( $K_{\downarrow}$ ), (b) specific humidity deficit ( $\Delta q$ ), (c) air temperature ( $T_{air}$ ), and (d) soil moisture deficit ( $\Delta\theta$ ). Additionally, (e) shows the connection between respiration ( $F_{res}$ ) and air temperature.

of the available data 100 times. This iterative process yields the final set of parameters, with medians determined alongside their associated uncertainties. In the context of photosynthesis, the parameters  $F_{pho,max,i}$  and  $G_2$  through  $G_6$  are subjected to fitting using data collected during the summer season, assuming relatively stable LAI. In contrast, the parameterization of respiration is recommended to encompass the entire year, as this approach prevents the overestimation of wintertime respiration rates.

To facilitate this parameterization process, it is essential to have access to observations of photosynthesis and respiration as well as key environmental variables, including air temperature, humidity, soil moisture, and incoming shortwave radiation. Additionally, accurate estimations of soil properties such as field capacity and wilting point are required to ensure the robustness of the parameterization procedure. In **Papers I and IV**, EC measurements obtained from various vegetated sites (lawn, urban forest) were used to apprehend the biogenic model parameters. In **Papers II and IV**, measurements at tree level from Helsinki were utilized for this purpose.

### 3.2.2 Yasso

Yasso is a soil carbon decomposition model (Tuomi et al., 2009; Liski et al., 2005), in which the rate of decomposition is influenced by both climatic conditions and the chemical composition of soil organic matter. The model requires either annual or monthly precipitation and air temperature, to drive its simulations. Yasso operates by simulating changes in carbon stock, considering the balance between the decomposition of soil organic matter and potential litter input into the system (Fig. 7). The decomposition rate in Yasso varies for four distinct carbon compound groups integrated into the model: compounds that are soluble in ethanol (E), compounds that are soluble in water (W), compounds that are hydrolysable in acid (A), and compounds that are neither soluble nor hydrolysable (N). Additionally, there is a mass flow directed towards recalcitrant humus (H). Litter input, which can consist of materials such as leaf litter, fine root litter, and woody litter (e.g., branches, stems, and coarse roots), can be incorporated into the model. The AWENH ratios are defined separately for the initial soil carbon pool and for the litter input. The parameters influencing the decomposition rates of various compounds are derived from extensive global litter decomposition measurements. In **Paper II**, version Yasso15 (Viskari et al., 2020) was used.

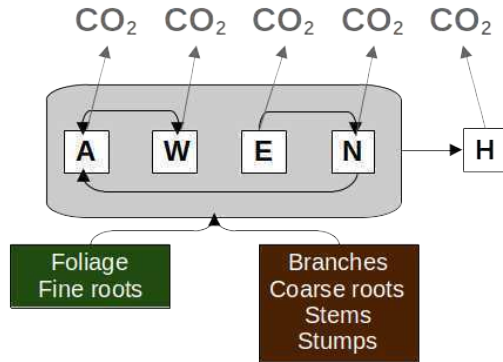


Figure 7: Flowchart of the Yasso model. Boxes represent the carbon compound groups: soluble in ethanol (E), or water (W), hydrolysable in acid (A), neither soluble nor hydrolysable (N) compounds, and recalcitrant humus (H), and arrows the exchange between them and towards CO<sub>2</sub> emitted from soil to the atmosphere. (Modified after Tuomi et al., 2011.)

### 3.3 Forcing data

Both the SUEWS and Yasso models rely on meteorological inputs as their primary forcing data. In the case of SUEWS, the prerequisite is that the meteorological data are situated within the inertial sublayer (ISL). These meteorological datasets can be procured either from direct observations or from reanalysis products.

In the context of simulating specific locations in Helsinki, **Papers I** and **II** made use of observations gathered during 2002–2016 from the SMEAR III station. In **Paper III**, the research employed the WFDE5 reanalysis dataset (Cucchi et al., 2021) derived from the European Centre for Medium-Range Weather Forecasts (ECMWF) atmospheric reanalysis (Hersbach et al., 2020) in Beijing in 2015–2016. In **Paper IV**, the study utilized the MET Nordic dataset (Nipen et al., 2020) for Helsinki. This dataset is available at hourly temporal resolution and 2.5 km spatial resolution. It comprises post-processed numerical weather prediction data from the MetCoOp Ensemble Prediction System (MEPS, Bengtsson et al., 2017; Müller et al., 2017), complemented by observations from various stations. Additionally, it includes post-processed data at a 1 km resolution. The dataset was further interpolated with a nearest neighbour approach to get forcing for each 250 x 250 m<sup>2</sup> simulation grid for years 2015–2019. For investigations concerning the climate conditions of the 2050s in the Helsinki region, adjustments were made according to the Representative Concentration Pathway (RCP) scenario RCP8.5, considering greenhouse gases and aerosols. These adjustments were undertaken as part of the work by Saranko et al. (2020) to produce the necessary meteorological forcing data. The spatial resolution used in this data match that of the MET Nordic dataset.

### 3.4 Surface characteristics

Surface cover fractions, as well as the heights of buildings and trees, were derived from high-resolution airborne lidar data, with a resolution of 2 m (Nordbo et al., 2015) in **Paper I** and at an even finer resolution of 1 m (StromJan, 2020) in both **Papers II** and **IV**. In **Paper I**, it was assumed that all low vegetation consists entirely of deciduous plants. Trees were categorized as 60% deciduous and 40% evergreen. This categorization was based on the assumption that street trees are half deciduous and forest trees in the region are 25% deciduous, a pattern observed in the southern coastal

region of Finland (Korhonen et al., 2015). In **Paper II**, all street trees were considered deciduous. For **Paper IV**, the classification of trees into evergreen or deciduous trees was determined using the Copernicus High-Resolution Layers with a 10 m resolution, which identifies the dominant leaf type (EEA, 2020). In **Paper III**, surface cover fractions were estimated based on aerial images with a 1 m resolution (Kokkonen et al., 2019).

### 3.5 Local Climate Zones (LCZs)

LCZs (Stewart and Oke, 2012) in Helsinki were categorized based on two publicly available datasets with a spatial resolution of 100 meters. The primary classification was derived from the European-level LCZ map (Demuzere et al., 2019). However, it lacked information for 8% of the grids in Helsinki, primarily due to some of the main islands being absent from this dataset. Therefore, the missing grid cells were supplemented using the global-level LCZ map (Demuzere et al., 2022). LCZs were then adjusted to the grid size of 250 x 250 m<sup>2</sup>, based on the dominant LCZ class within each grid. As a result, Helsinki was classified into eight distinct LCZ classes (see Table 1).

### 3.6 Statistics

The performance of the models was assessed using standard statistical metrics, including a Pearson correlation coefficient ( $r$ ), root-mean-square error (RMSE) and its normalization (nRMSE), mean absolute error (MAE), and normalized mean bias error (nMBE). In **Papers I** and **III**, nRMSE was calculated using the maximum value of the observation and minimum value of the model. In **II**, the normalization of nRMSE and nMBE were done with the maximum and minimum values of the observations.

Table 1: Local Climate Zones in Helsinki.

LCZ	Name	Fraction	Description
2	<i>Compact midrise</i>	2.7%	Dense mix of midrise buildings (3–9 stories). Few or no trees. Land cover mostly paved.
5	<i>Open midrise</i>	19.6%	Open arrangement of midrise buildings (3–9 stories). Abundance of pervious land cover (low plants, scattered trees).
6	<i>Open lowrise</i>	16.2%	Open arrangement of low-rise buildings (1–3 stories). Few or no trees. Abundance of pervious land cover.
8	<i>Large lowrise</i>	15.9%	Open arrangement of low-rise buildings (1–3 stories). Few or no trees. Land cover mostly paved.
9	<i>Sparsely built</i>	1.1%	Sparse arrangement of small or medium-sized buildings in a natural setting. Abundance of pervious land cover.
A	<i>Dense trees</i>	25.4%	Heavily wooded landscape of deciduous and/or evergreen trees.
B	<i>Scattered trees</i>	6.5%	Lightly wooded landscape of deciduous and/or evergreen trees.
D	<i>Low plants</i>	12.6%	Featureless landscape of grass or herbaceous plants/crops. Few or no trees.

## 4 Results

### 4.1 Model evaluation

#### 4.1.1 Neighbourhood-scale

Evaluating the newly developed CO<sub>2</sub> module using EC observations in urban areas necessitates the estimation of both biogenic and anthropogenic components. This is particularly important because the neighbourhood-scale sites examined in **Papers I** and **III** were influenced by substantial anthropogenic emissions. The net CO<sub>2</sub> exchange modelled with SUEWS demonstrated a strong agreement with the EC observations at hourly, diurnal, and annual levels, both in Helsinki and Beijing. The summer season, when vegetation is most active, provides the optimal time to evaluate the biogenic CO<sub>2</sub> module (Fig. 8).

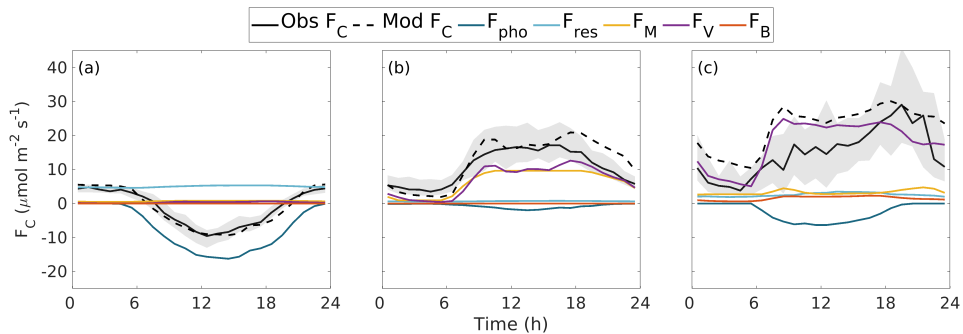


Figure 8: Median (lines) diurnal behavior of measured and modelled CO<sub>2</sub> exchange ( $F_C$ ,  $\mu\text{mol m}^{-2} \text{s}^{-1}$ ) and its components at (a) Kumpula vegetation (Ku3) sector, (b) at Tornii, and (c) at Beijing for June to August. The evaluation years are 2012 for Kumpula and Tornii, and 2016 for Beijing. CO<sub>2</sub> emissions/sink from photosynthesis ( $F_{pho}$ ), respiration ( $F_{res}$ ), human metabolism ( $F_M$ ), traffic ( $F_V$ ), and buildings ( $F_B$ ). Gray areas show the 25th/75th percentiles of the measured  $F_C$ . Figure adapted from **Papers I** and **III**.

In **Paper I**, the Kumpula site was divided into three sectors, each simulated and analyzed separately. Among these sectors, the Ku3 sector, characterized by 31% grass

surfaces and 28% tree cover, provided the most accurate representation of urban biogenic CO<sub>2</sub> exchange. Consequently, the biogenic model was calibrated specifically for this sector. For independent evaluations, data from the years 2006 to 2011 were utilized for parameter fitting, with the independent year 2012 serving as the evaluation period. In this sector, the model demonstrated its optimal performance, particularly during the summer months, as evident from the diurnal medians (Fig. 8a). While perfect alignment of hourly values was not expected due to potential measurement errors associated with EC, the model exhibited strong performance during summer in the Ku3 sector, with a high  $r$  value of 0.84, and relatively low values for RMSE (2.93  $\mu\text{mol m}^{-2} \text{s}^{-1}$ ), nRMSE (0.066), and MAE (0.06) (see Table 2). In contrast, during other seasons within the vegetated Ku3 sector, the exchange values were considerably smaller, and the model’s performance comparatively poorer. The  $r$  values ranged from 0.17 to 0.48 (spring–autumn), and MAE values ranged from 0.35 to 1.11  $\mu\text{mol m}^{-2} \text{s}^{-1}$  (winter–spring). Notably, wintertime respiration values were slightly overestimated. In other sectors within Kumpula, the model successfully captured the combined effects of anthropogenic activities and biogenic exchange during the summer months. The correlations were poorer than for the Ku3 sector, with  $r$  values of 0.67 (Ku1) and 0.31 (Ku2). Although the  $r$  value was lowest for Ku2, the MAE value was better (0.1  $\mu\text{mol m}^{-2} \text{s}^{-1}$ ) compared to Ku1 (1.46  $\mu\text{mol m}^{-2} \text{s}^{-1}$ ), possibly due to disruptions from nearby buildings in the Ku1 sector.

Table 2: Statistics at EC sites in Kumpula, Tornii, and Beijing. The statistics are a root-mean-square error (RMSE,  $\mu\text{mol m}^{-2} \text{s}^{-1}$ ), a normalized root-mean-square error (nRMSE), a Pearson correlation coefficient ( $r$ ), and mean absolute error (MAE,  $\mu\text{mol m}^{-2} \text{s}^{-1}$ ) from summer seasons only.

Site	RMSE	nRMSE	$r$	MAE	N
Ku1	1.85	0.048	0.67	1.46	372
Ku2	3.00	0.040	0.31	0.10	905
Ku3	2.93	0.066	0.84	0.06	1917
Tornii	5.27	0.061	0.63	0.24	2160
Beijing	13.99	0.203	0.43	11.18	1097

In contrast, the model’s performance in the city centre location, Tornii (**Paper I**), was primarily influenced by anthropogenic activities (Fig. 8b), making it challenging to isolate the influence of vegetation. The observed net CO<sub>2</sub> exchange did not exhibit morning or evening rush hour patterns during the summer, whereas the simu-

lated traffic emissions indicated peak levels during these hours. Although these rush hour peaks are more pronounced in the winter, SUEWS can only incorporate a static diurnal profile, possibly leading to a mismatch with the summer traffic patterns. Consequently, the simulated net CO<sub>2</sub> exchange was overestimated during rush hours and evenings, resulting in a reduced  $r$  value of 0.64 during the summer. Although the traffic profile more accurately represented wintertime traffic, the observed CO<sub>2</sub> exchange experienced a delay due to weak turbulent mixing in the early morning, resulting in similar  $r$  values of 0.65 in the winter months. Nevertheless, considering all these factors, SUEWS demonstrated a good model performance when compared to EC measurements in Helsinki.

In Kumpula (**Paper I**), the modelled annual CO<sub>2</sub> emissions, at 1440 g C m<sup>-2</sup> y<sup>-1</sup>, slightly exceeded the observed gap-filled value of 1414 g C m<sup>-2</sup> y<sup>-1</sup>, by a modest 2% (Fig. 9). In the city center, the model estimated annual emissions of 4640 g C m<sup>-2</sup> y<sup>-1</sup>, which was 3% higher than the gap-filled observed value of 4507 g C m<sup>-2</sup> y<sup>-1</sup>. These overestimations were minimal, especially when taking into account the inherent uncertainty associated with EC measurements, which can range from 15% to 60% over vegetated ecosystems (Baldocchi, 2003). Additionally, addressing the overestimation of respiration during winter could potentially lead to slight reductions in the estimations, as the vegetation might act as a CO<sub>2</sub> sink over the year.

In **Paper III**, certain discrepancies between observations and the model, particularly during morning hours were seen, likely arising from the estimation of traffic emissions in Beijing (Fig. 8c). Furthermore, the model domain remained a constant 1 km circle around the EC site, while EC observations have a variable footprint dependent on wind direction and atmospheric stability (Liu et al., 2012). Consequently, this resulted in poorer model performance than in **Paper I**, with a relatively low  $r$  value of 0.42 and high nRMSE value (0.2) during summer. Additionally, the simulated latent heat flux ( $Q_E$ ) was evaluated against EC measurements, as it provided a more direct connection to vegetation. During the summer, the model demonstrated improved performance in estimating  $Q_E$ , with an  $r$  value of 0.65 and an nRMSE of 0.12.

The impact of footprint size on annual cumulative totals became evident when comparing simulations with gap-filled EC observations, especially for Beijing in **Paper III**, where SUEWS overestimated the annual values by approximately 15% (Fig. 9). The simulated value amounted to 8.6 kg C m<sup>-2</sup> y<sup>-1</sup>, whereas the observed gap-filled value was 7.5 kg C m<sup>-2</sup> y<sup>-1</sup>. However, altering the model domain radius from 500 to 1500

m resulted in annual values of  $F_C$  ranging from 7.4 to 8.7 kg C m<sup>-2</sup> y<sup>-1</sup>. A smaller radius corresponded to reduced emissions from traffic, aligning more closely with the gap-filled EC observations.

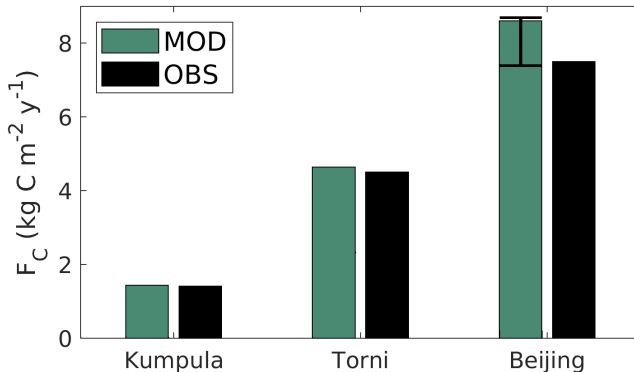


Figure 9: Annual sums of modelled (green) and gap-filled EC (black)  $F_C$  at EC sites in Kumpula, Tornii, and Beijing. The whisker describes how much  $F_C$  varies with the varying model domain in Beijing.

#### 4.1.2 Street trees and soil

In **Paper II**, measurements conducted on street trees were used to evaluate the model’s performance. Initially, measurements obtained using a portable gas exchange sensor (Riikonen et al., 2011) were used to assess how leaf-level exchange responded under varying environmental conditions. These measurements also helped to derive new parameters related to conductance that specifically represent street trees. Subsequently, as photosynthesis and transpiration are interconnected through stomata, the model’s performance was evaluated with transpiration estimations obtained using sap flow sensors (Riikonen et al., 2016).

Simulated transpiration was found to be sensitive to the maximum surface conductance value ( $g_{i,max}$ , see Eq. (3)), as high values led to unrealistic soil drying. The originally used parameter for deciduous trees (11.7 mm s<sup>-1</sup>, **Paper I**) was not suitable for the street trees in **Paper II**, as the value was more appropriate for heavily irrigated areas (Järvi et al., 2011). Instead, values of 3.1 mm s<sup>-1</sup> for *Tilia* and 8.7 mm s<sup>-1</sup> for *Alnus*, based on prior literature, were chosen to better match the site conditions.

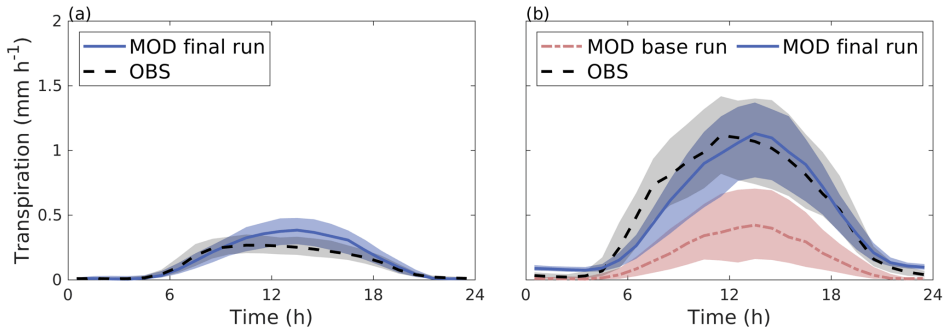


Figure 10: Median diurnal cycle of modelled transpiration (solid blue line) and transpiration estimated from observed sap flow (dashed black line) from June to August 2008–2011 for (a) the Tilia site and (b) the Alnus site. In panel (b), the red line represents the model simulation without an additional water source (the base run). The shaded areas are the 25th/75th percentiles. Figure adapted from **Paper II**.

At the Tilia site, the model performed well against transpiration estimated from observed sap flow (Fig. 10a). However, at the Alnus site, the water available for trees was not enough to support high transpiration amounts in the base run (see Fig. 10b). While SUEWS accurately represented surface-level water dynamics, with soil moisture nRMSE between 0.16–0.23, it became evident that street trees needed additional water sources beyond the surface soil layer. It was assumed that these trees rely on unaccounted-for water sources, possibly deeper soil layers not considered in SUEWS. After including an estimation of these sources, the model results aligned well with transpiration estimates from sap flow measurements (see Fig. 10b), with nRMSE values ranging from 0.11 to 0.34 between the different years. These results highlighted that the model was highly sensitive to the urban water balance. For instance, incorporating multiple soil layers would provide trees with greater access to water compared to grasses with shorter root systems.

While SUEWS is capable of providing an estimation on respiration, it mainly represents an average rate for urban ecosystems, while lacking any consideration of the historical soil conditions or structure. Thus, an evaluation of the soil carbon model Yasso was conducted, with a particular focus on its applicability to simulate urban soils. In **Paper II**, Yasso was used to estimate the soil carbon pools in three different soil types on newly established street soils implemented in 2002.

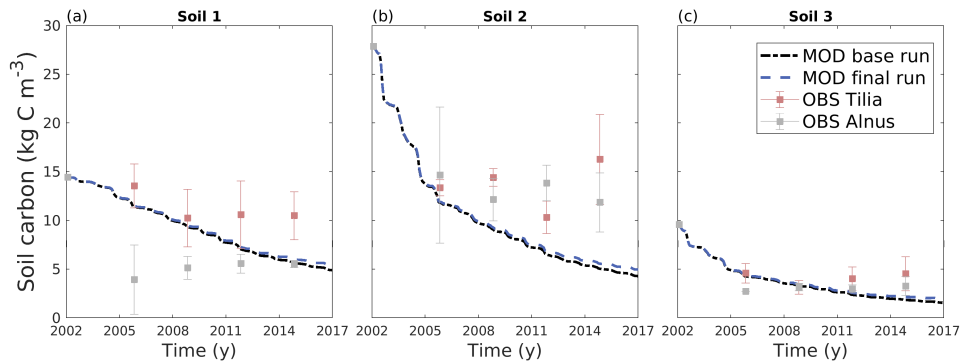


Figure 11: Monthly soil carbon stock modelled using Yasso without fine root litter input (dashed black line) and with fine root litter input (dashed blue line) from 2002 to 2016, and measured average loss-on-ignition-based soil carbon stock estimations ( $\pm$  SD) for the three studied soil types at the Tilia site (red dots) and the Alnus site (gray dots). Figure adapted from **Paper II**.

Over the period from 2002 to 2016, there was a notable decline in the soil carbon pool (Fig. 11). The model performed the best for soil 3 at both sites. In contrast, the model consistently underestimated the soil 2 carbon pool, while its performance in soil 1 exhibited mixed results. The nRMSE values ranged from 0.59 to 0.88 at the Tilia site, indicating relatively better model performance compared to the Alnus site, where nRMSE values span from 0.73 to 1.36. In terms of nMBE, the Tilia site also showcased a more favorable overall performance, with values ranging from -0.91 to -0.75. Furthermore, the influence of decomposing fine roots on the model outcomes remained minimal and scarcely detectable until the later stages of the simulation period. This was evident from the negligible deviation observed in the model run with fine root litter input when compared to the base run without root litter. However, the statistical values should be interpreted with caution, as the assessment relied on merely four measurement points in time. Nevertheless, the model performance was good considering the lack of knowledge regarding the actual AWENH-fractions at the time of street construction. These street soil estimates were notably lower ( $1.7\text{--}5.7\text{ kg C m}^{-2}$ ) than those previously recorded in parks within Helsinki ( $10.4\text{ kg C m}^{-2}$ ; Lindén et al., 2020) or in forest soils in Finland ( $6.3\text{ kg C m}^{-2}$ ; Liski et al., 2006). However, these street soils were composed of structural soils, consisting of roughly two-thirds stones and the remaining third was fine soil, thus the estimates were in a reasonable range. Although

Yasso was not originally designed for urban soils, these results emphasize its potential for adaptation to this environment. Nonetheless, a more comprehensive evaluation on urban soils is instrumental to refining Yasso for broader city-wide applications. One of the main challenges when using Yasso in urban areas is the necessity for soil history information. This data might be entirely absent or exhibit significant variations, making it challenging to generalize the results.

### 4.1.3 Applicability of SUEWS for simulating urban CO<sub>2</sub> exchange

SUEWS enables the investigation of biogenic CO<sub>2</sub> exchange at various scales, providing support for both urban measurements and urban planners. Nevertheless, it is essential to acknowledge that the methods employed in this study have their limitations. Urban models inevitably simplify the intricate urban systems they aim to represent. Urban environments are notably complex, featuring diverse plant species, soil types, and land uses. Consequently, the model's simplifications may not fully capture this intricacy.

In addition, the modelling approach in this thesis, while valuable, might not be seamlessly applicable to all urban settings, especially those with limited data or modelling resources. This limitation becomes pronounced when dealing with areas where precise vegetation mapping for the classification of trees and other vegetation is unavailable. The selection of model parameters introduces a degree of uncertainty, and one potential solution lies in the development of a climate-dependent lookup table. In the absence of precise measurements, modelling often entails educated estimations, which can lead to inaccuracies. Furthermore, it is essential to acknowledge that the CO<sub>2</sub> module's applicability has not been tested in tropical climates, where the seasonal patterns of biogenic CO<sub>2</sub> exchanges diverge from those studied here. When comparing models with measurements, it is crucial to take into account the source area, particularly in the case of CO<sub>2</sub>, as its emissions are influenced by more localized factors compared to variables such as water or heat.

However, SUEWS remains an evolving model as new research unfolds in the field of urban meteorology. This thesis highlighted that the CO<sub>2</sub> uptake is highly sensitive to the urban water balance (**Papers II and IV**). For instance, incorporating multiple soil layers would provide trees with greater access to water compared to grasses with shorter root systems. Additionally, the current respiration model solely relies on air temperature, but future improvements could modify it based on soil water availabil-

ity, further enhancing the model’s accuracy. The uncertainty limits of respiration and photosynthesis parameters were examined in **Paper I**, revealing that the variability in respiration parameters was three times greater than in photosynthesis parameters. This difference was partially attributed to the wider range in measured respiration, potentially influenced by varying soil moisture conditions. Some urban models, as indicated by Stagakis et al. (2023b), have already integrated soil moisture measurements into their respiration calculations. Given that SUEWS is an urban water balance model, the incorporation of modelled soil water availability into the respiration calculations is a feasible prospect. Currently, respiration parameters are parameterized for specific types of urban ecosystems, such as irrigated or non-irrigated lawns. However, there is potential to explore a more detailed representation within the model in the future.

Lastly, employing urban land surface models to assess the potential influence of future climate conditions on the CO<sub>2</sub> exchange presents challenges (**Paper IV**). The model relies on parameters obtained from measurement data in the current climate, assuming that the environmental relationships observed during that period will persist in the coming decades. However, this introduces uncertainties, considering the unknown adaptability of plants to future changes. Additionally, since urban land surface models may not necessarily account for the diverse soil types within a city, future predictions may overlook this variability. Nevertheless, due to the non-linear nature of these relationships, making predictions based on them can provide greater accuracy than using linear responses.

## 4.2 CO<sub>2</sub> exchange of street tree plantings

Throughout the extended study period in **Paper II**, from 2003 to 2031, both models were used to estimate the CO<sub>2</sub> exchange of street trees (using SUEWS) and soil carbon emissions (using Yasso). The Viikki street tree site included two streets, each with their own tree species. Figure 12 shows the average behaviour of the different species.

The estimated annual CO<sub>2</sub> uptake via photosynthesis varied across years 2003–2031, ranging on average from -3.1 to -12.1 kg C y<sup>-1</sup> per tree (Fig. 12). Simultaneously, tree respiration spanned from 1.5 to 5.7 kg C y<sup>-1</sup> per tree. These CO<sub>2</sub> exchange processes resulted in a consistent net CO<sub>2</sub> sink for the trees, with average values ranging from -1.5 to -6.6 kg C y<sup>-1</sup> per tree. These estimates, however, appeared lower than those obtained through alternative methods for assessing carbon sequestration by street trees

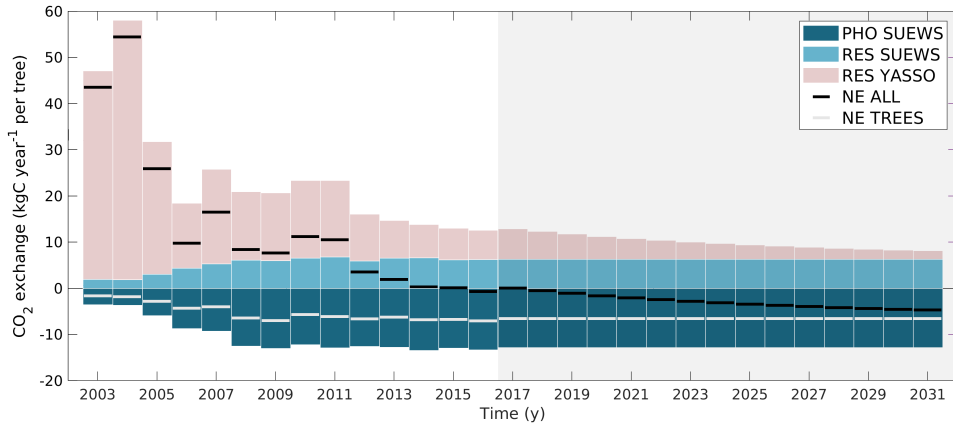


Figure 12: Estimated annual net exchange (NE ALL, black) of street tree plantings and only for trees (NE TREES, gray), CO<sub>2</sub> uptake by photosynthesis (PHO SUEWS, dark blue), emissions from tree respiration simulated with SUEWS (RES SUEWS, light blue), and emissions from soil respiration simulated with Yasso (RES Yasso, light rose) at the Tilia site. The gray area separates the actual simulations from the estimations made with mean meteorological forcing for the future climate. Here, positive values indicate a release of CO<sub>2</sub> to the atmosphere and negative values indicate uptake from the atmosphere. Figure adapted from **Paper II**.

in Europe. For instance, in Italy, street trees were reported to sequester carbon from -12.1 to -17.4 kg C y<sup>-1</sup> per tree (Russo et al., 2014). In Portugal, street trees were estimated to sequester a significantly higher amount, approximately -43.1 kg C y<sup>-1</sup> per tree (Soares et al., 2011). However, the trees in these studies were situated in a warmer temperate zone, likely being more mature, which could potentially account for their enhanced sequestration capacity compared to the younger trees examined in **Paper II**.

While individual street trees consistently acted as CO<sub>2</sub> sinks, it is important to consider the entire street tree planting, including the estimated 25 m<sup>2</sup> planting pocket surrounding each tree. Soil respiration varied on average from 57.1 kg C y<sup>-1</sup> per tree two years after construction to 1.7 kg C y<sup>-1</sup> per tree after 30 years.

When assessing the net exchange (NE) for the entire street tree planting, it became evident that it takes time for the collective system to transition into a net CO<sub>2</sub> sink.

On average, this transition occurred after approximately 12 years. The overall NE was estimated to be  $-4.4 \text{ kg C y}^{-1}$  per tree after 30 years. The initial loss of carbon from soil was substantial because manufactured soils can contain a significant amount of carbon that is released into the atmosphere. However, if these soils were used elsewhere, these emissions would still eventually enter the atmosphere. Because of this initial peak, it takes more than 30 years for the cumulative NE to turn negative. These results highlight the importance of including soil into studies focusing on urban  $\text{CO}_2$  sinks, with **Paper II** being among the first studies showing this.

### 4.3 Impact of surface cover on biogenic $\text{CO}_2$ exchange in a changing climate

In **Paper I**, the city centre of Helsinki was simulated using SUEWS, covering an area of approximately  $7 \times 9 \text{ km}^2$  with a spatial resolution of  $250 \times 250 \text{ m}^2$ . The net annual exchange in this region amounted to approximately  $81.8 \text{ kt C}$ , with a contribution of  $2.8 \text{ kt C}$  from biogenic processes. Here, respiration surpassed photosynthesis in overall magnitude on an annual level. Anthropogenic emissions were divided into 61% from vehicle emissions and 39% from humans, highlighting the substantial impact of human respiration.

The aim in **Paper IV** was to expand this modelling domain to encompass the entirety of Helsinki (see Fig. 13a), while mainly focusing on the biogenic  $\text{CO}_2$  exchange. The net  $\text{CO}_2$  uptake was approximately  $-36.3 \pm 7.7 \text{ kt C y}^{-1}$  for years 2015–2019.

The model exhibited a comprehensive capability in integrating energy, water, and  $\text{CO}_2$  exchanges. Within the biogenic  $\text{CO}_2$  module, it can account for a range of local urban factors, including variations in temperature within the RSL (Fig. 13b), soil moisture levels, and irrigation patterns. Temperature patterns within the RSL were influenced not only by anthropogenic activities but also by the distribution of impervious surfaces and vegetation cover. This resulted in variations in simulated 2 m air temperature across each grid. In the most extreme cases, the annual temperature differences between grids could reach up to  $5^\circ\text{C}$  (Fig. 13b). Local soil moisture conditions were significantly affected by increased runoff, resulting from extensive paved surfaces and the potential excess of irrigation practices typically observed in suburban areas. These conditions had a significant impact on surface conductance.

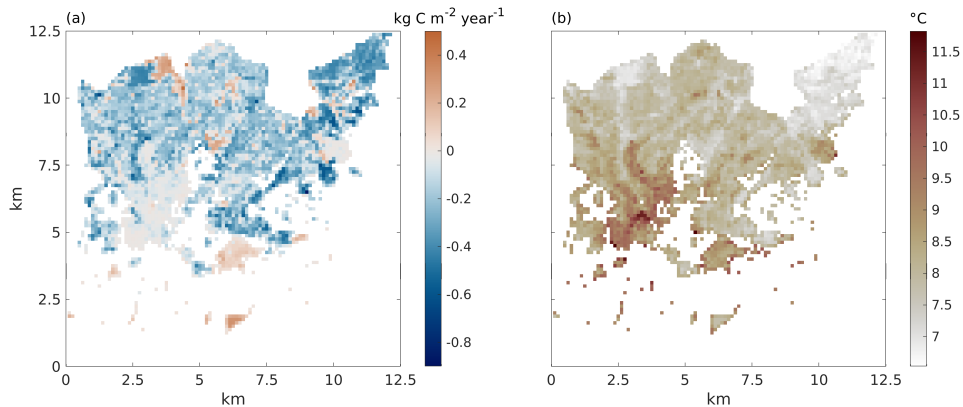


Figure 13: Average (a) annual net exchange ( $F_{C,bio}$ ), and (b) mean 2 m air temperature in Helsinki in 2015–2019. Figure adapted from **Paper IV**.

The results derived from city-wide simulations (Fig. 13a) were further categorized based on the Local Climate Zone classification (Fig. 14). Within *dense trees* zone (LCZ A), the median CO<sub>2</sub> uptake was the highest at  $-0.3 \text{ kg C m}^{-2} \text{ y}^{-1}$ , while *scattered trees* (LCZ B), *open midrise* (LCZ 5), and *open lowrise* (LCZ 6) zones all exhibited comparable median values, ranging from  $-0.17$  to  $-0.19 \text{ kg C m}^{-2} \text{ y}^{-1}$ . While *dense trees* and other rural areas were the strongest sinks ( $-19 \text{ kt C y}^{-1}$ ), urban neighbourhoods made a substantial contribution to Helsinki’s CO<sub>2</sub> sinks ( $-16 \text{ kt C y}^{-1}$ ), accounting for 47% of the total, as they covered 56% of the city’s area. These findings underscore the significance of vegetation beyond urban forests in contributing to these sinks.

Areas with only low vegetation (LCZ D), such as lawns, typically experienced drying during the summer months (**Paper IV**). This resulted in decreased photosynthetic activity and transformed these regions into net CO<sub>2</sub> sources on an annual level. In contrast, trees, while also affected by dry conditions, displayed higher resilience. This was attributed to their capacity to access water sources due to their deeper 1 m soil layer, which surpassed the capabilities of shallower-rooted grasses. Consequently, the magnitude of CO<sub>2</sub> uptake was found to be closely correlated with the extent of tree cover within the study area.

In addition, SUEWS was applied to model future local climate and CO<sub>2</sub> exchange. Under the RCP8.5 projection in Helsinki for the 2050s, the model estimated an 11% increase in CO<sub>2</sub> uptake when compared to climate in 2015–2019. This modest increase

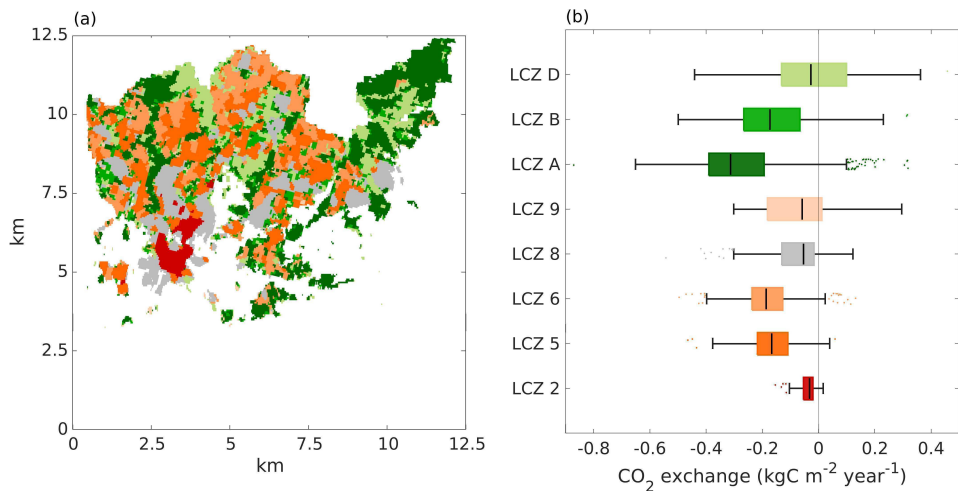


Figure 14: (a) Local Climate Zone (LCZ) map of Helsinki with 100 m resolution (Demuzere et al., 2019, 2022) and each simulated grid grouped into LCZs in the (b) box plot of biogenic CO<sub>2</sub> exchange ( $F_{C,bio}$ ) for 2015–2019 climate. Figure adapted from **Paper IV**.

was attributed to multiple factors influencing CO<sub>2</sub> exchange dynamics. Elevated temperatures extended the growing season both in spring and autumn, leading to an overall increase in photosynthetic uptake. In contrast, prolonged dry periods during summer months had the opposite effect, reducing photosynthesis during these periods. In addition, respiration was slightly higher overall due to warmer temperatures. The scenario also had varying results based on the LCZs. Urban neighbourhoods were predicted to warm approximately 1°C more than the vegetated zones, increasing their temperature differences even further. The *dense trees* zone was particularly affected by dry conditions decreasing on average 1  $\mu\text{mol m}^{-2} \text{s}^{-1}$  from June to August, while urban neighbourhoods could mitigate this effect through irrigation practices. In addition, *low plants* were becoming even more reliant on irrigation.

#### 4.4 Offset of biogenic CO<sub>2</sub> exchange

The newly developed biogenic CO<sub>2</sub> exchange module was capable: 1) to determine the relative importance of biogenic components compared to anthropogenic emissions

near EC towers, thereby contributing to reducing measurement uncertainties, and 2) to estimate the overall CO<sub>2</sub> offset at a city-wide scale.

In **Papers I** and **III**, the areas surrounding EC towers were observed as net sources of CO<sub>2</sub> over the course of a year, with annual totals amounting to 1.4, 4.5, and 7.5 kg C m<sup>-2</sup> y<sup>-1</sup> for Kumpula, Tornii, and Beijing, respectively (Fig. 9). These emissions primarily originated from anthropogenic activities, although biogenic components also contributed to annual emissions. This was attributed to respiration exceeding the amount of CO<sub>2</sub> absorbed by photosynthesis, resulting in a net biogenic source.

However, the estimation of source areas as either sources or sinks was highly sensitive to the selected model parameters. For instance, the respiration parameters used in **Paper I** were based on summertime measurements, resulting in a high  $a$  parameter in Eq. (10). This, in turn, led to an overestimation of respiration during the winter months. Although SUEWS performed well during the growing season, this overestimation during the winter resulted in these areas being sources of CO<sub>2</sub> on an annual basis, despite their potential to act as sinks. In **Paper III**, the source area around the EC tower was also a source of CO<sub>2</sub>, however, this was primarily attributed to the extent of low vegetation and soil respiration in comparison to the canopy cover.

Nevertheless, the relative importance of biogenic components compared to anthropogenic emissions near EC towers holds more significance on hourly and daily levels than on an annual basis. Biogenic CO<sub>2</sub> exchange exhibited significant seasonal variations, peaking during the summer months. For example, in June, daily CO<sub>2</sub> uptake could even surpass anthropogenic emissions, as evidenced in Kumpula, where the uptake could be over four times higher than emissions on a daily basis. However, other locations, such as Tornii and Beijing, exhibited more modest daily offsets in June, at -7% and -1%, respectively. Furthermore, SUEWS accurately captured the diurnal variations in CO<sub>2</sub> uptake. For instance, in Kumpula, at noon in June, the overall net exchange turned negative, indicating that the vegetation offset all of the emissions. In contrast, in Tornii and Beijing, the offsets were lower at -16% and -26%, respectively. **Papers I** and **III** demonstrated the usability of SUEWS in the source partitioning of CO<sub>2</sub> eddy covariance measurements, which is critical for urban CO<sub>2</sub> monitoring networks.

Annually, the effect of vegetation surfaces around urban EC sites is marginal, with the potential to either emit or sequester CO<sub>2</sub>. Compared to other methods used in

cities, the biogenic components have been estimated to offset annually between -1.5 and -4.5% in Minneapolis-Saint Paul, US (Menzer and McFadden, 2017), -0.5% in Toulouse, France (Goret et al., 2019), and -1.4% in Singapore (Velasco et al., 2016), while acting as a source of 4.4% in Mexico City (Velasco et al., 2016) and 1.3% in Basel, Switzerland (Stagakis et al., 2023a). In the case of Mexico city, it was suggested that the source was due to soil respiration limiting the potential of carbon sequestration.

City-wide simulations, as presented in **Paper IV** for Helsinki, introduced new parameters and placed specific focus on wintertime respiration and annual balances. The offset accounted for approximately 7% when compared to the anthropogenic emissions of 508.8 kt C annually. However, this offset also showed seasonal variation. On average, during the summer months, the offset amounted to approximately 42%. In contrast, in the winter season, respiration could even contribute to emissions, accounting for up to 12%. Comparing these findings to other cities, Boston, US, reported a smaller offset of 2.1% (Hardiman et al., 2017), while Florence, Italy, estimated a 6.2% offset (Vaccari et al., 2013). Inevitably, these percentages are significantly influenced by the magnitude of anthropogenic emissions produced by each city, rather than being solely determined by the extent of vegetation within the city.

## 5 Conclusions

Urban green areas significantly influence the exchange of CO<sub>2</sub> in urban environments. This thesis aimed to assess the contribution of biogenic CO<sub>2</sub> exchange to anthropogenic emissions for two primary reasons: 1) Biogenic components introduce uncertainties in measuring anthropogenic emissions, and 2) urban vegetation and soil can offset part of these emissions. This thesis involved the development of the CO<sub>2</sub> module within the urban land surface model SUEWS and addressing the following questions:

1. Is the urban land surface model SUEWS applicable to simulate urban CO<sub>2</sub> exchange?
2. What is the role of soil in CO<sub>2</sub> exchange of newly planted street trees?
3. How does biogenic CO<sub>2</sub> exchange vary with different surface covers in Helsinki, and how will this be changed by climate change?
4. To what extent can biogenic CO<sub>2</sub> exchange offset anthropogenic emissions in different scales?

In **Paper I**, the empirical canopy-level photosynthesis and ecosystem-level respiration models were included within the SUEWS model, as well as a simplified bottom-up inventory model for anthropogenic emissions. The CO<sub>2</sub> module demonstrated its effectiveness against several measurements. The net CO<sub>2</sub> exchange was evaluated against three urban EC observations in **Papers I** and **III**, while **Paper II** evaluated the simulation of street tree transpiration using local measurements. In addition to SUEWS, the soil carbon model Yasso was evaluated against street soil measurements in **Paper II**. SUEWS relies on meteorological data, and its physiological processes depend on these inputs. Incorporating urban-specific water balance offers advantages in simulating biogenic CO<sub>2</sub> exchange, considering urban processes like runoff and irrigation. However, parameter selection for each simulation domain requires careful attention. In addition to the water balance, SUEWS simulates 2-meter local air temperatures, influencing the estimation of photosynthesis and respiration. This integration represents a step towards accounting for the urban heat island effect on urban greenery.

The thesis focus ranged from specific street trees (**Paper II**) to neighbourhood-scale simulations around EC sites (**Papers I** and **III**), culminating in city-wide simulations for Helsinki (**Paper IV**). While individual street trees consistently functioned as

carbon sinks, street tree plantings, including planting pockets, initially emitted CO<sub>2</sub>, transitioning into carbon sinks approximately 12 years after construction. These results highlight the importance of including soil in the assessment when estimating CO<sub>2</sub> sinks from urban vegetation.

In **Paper IV**, the city-wide simulations in Helsinki were used to assess the contribution of various land cover types, connecting the results to Local Climate Zones (LCZs). The CO<sub>2</sub> sinks show variation across LCZs, with *dense forest* having the highest sink capacity and the downtown area showing the lowest. Nonetheless, the larger expanse of urban neighbourhoods makes a substantial contribution to the city-wide net sink, as approximately half of the CO<sub>2</sub> sinks are located outside of forested areas. Additionally, the city-wide simulations were used to estimate the 2050s climate with the RCP8.5 scenario. In this scenario, an 11% increase in carbon sequestration was estimated. The relatively modest increase can be attributed to the intricate interplay of multiple factors. Elevated temperatures affected the timing of leaf-on and leaf-off in vegetation, while extended dry periods led to drier soil conditions. LCZs responses to the RCP8.5 scenario varied, as urban neighbourhoods simultaneously warmed more than vegetative zones, as well as mitigated dryness with irrigation. Conversely, urban forests were more susceptible to these changing conditions. Furthermore, the impact on low vegetation types, such as lawns, which were already sensitive to dry conditions in the current climate, was expected to intensify in the future, making them increasingly reliant on irrigation.

This thesis demonstrated the usability of SUEWS to distinguish between different components of net CO<sub>2</sub> exchange measurements obtained using EC. The biogenic components could either completely counterbalance emissions or mitigate around a quarter of the emissions, particularly during daytime in the summer, as estimated in Beijing (**Paper III**). These variations were attributed to discrepancies in anthropogenic activity levels and vegetation density at each specific site, highlighting the need for distinct simulations tailored to individual urban EC sites. With the city-wide simulations in Helsinki, the annual offset was estimated at 7%, with a peak of 42% during the summer.

Overall, this thesis has limitations arising from the need to simplify the modelling of complex urban environments. While the SUEWS model itself has room for improvement, it is important to note that SUEWS is an evolving model. Thus, opportunities remain to further enhance the model's capacity to accurately simulate CO<sub>2</sub> exchanges in diverse urban settings across the globe. However, it is essential to emphasize that

achieving these improvements requires the availability of open-access measurements from cities around the world. Lastly, to enhance SUEWS' accessibility, it is part of UMEP (Urban Multi-scale Environmental Predictor, Lindberg et al., 2018), a tool operating within the QGIS (Quantum Geographic Information System) environment. The developed CO<sub>2</sub> module is currently in the process of integration into the UMEP system.

Together, these four papers bring further knowledge on urban biogenic CO<sub>2</sub> exchanges, with a specific focus on how soil and land cover influence CO<sub>2</sub> sinks. The application of SUEWS holds promise for the usage around urban EC towers as well as for estimating city-wide offsets. Furthermore, city-wide estimations can be invaluable for cities aiming for carbon neutrality, allowing them to consider their carbon offsets. In addition, these results underscore the importance of urban planning that incorporates green infrastructure to promote sustainability and resilience in cities facing the challenges of a changing climate.

## 6 Review of papers and the author’s contribution

This thesis comprises four papers that encompass model development, evaluation, and real-world application (Fig. 15), with the author playing a substantial role in all facets of the research. The author is exclusively responsible for the summary section of this thesis.

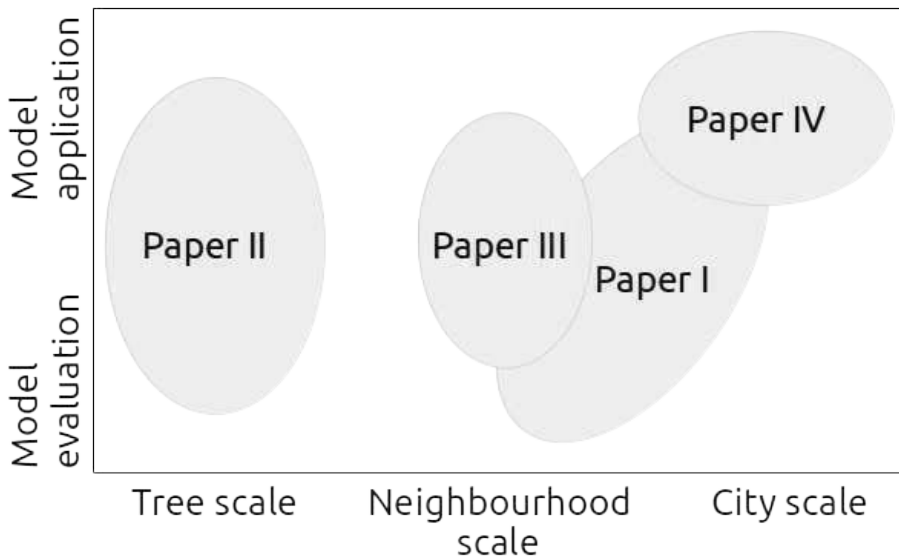


Figure 15: An overview of papers covering various scales, including model evaluations that utilize observations and applications of the evaluated models. **Papers I** and **III** focus on the neighbourhood-scale around EC observations, while in **Paper I** small scale spatial run was made within the city centre of Helsinki. **Paper II** focuses on the development of the module in street tree scale, while also estimating the whole street tree plantings sinks for 30 years. **Paper IV** focuses on spatial modelling of CO<sub>2</sub> for the whole city of Helsinki.

**Paper I** focuses on the development of the CO<sub>2</sub> module into the SUEWS model. The primary objective was to evaluate the model’s performance by comparing it against eddy covariance observations. The author contributed in developing the model code, design of the simulations, executing model runs, and generating a few of the figures. Furthermore, the author contributed collaboratively with all co-authors to write and

review the manuscript.

**Paper II** focuses into the examination of street tree CO<sub>2</sub> dynamics including the trees and soil beneath in Helsinki. This investigation involved the utilization of two models, SUEWS and Yasso, the evaluation of their performance against measurements from two test streets, and the estimation of the carbon balance of newly planted trees. The author contributed in developing a new parameterization specifically tailored for street trees. The author was responsible for the design, preparation, and execution of the simulations. The author wrote the manuscript with contributions from all co-authors.

**Paper III** extends the research scope to assess the applicability of the newly developed CO<sub>2</sub> module in Beijing, China. The author actively participated in the conceptualization of the study and contributed to the design of the simulations. Furthermore, the author played a collaborative role with all co-authors in the preparation and completion of the manuscript.

**Paper IV** shifts the investigation focus to explore the spatial variability of CO<sub>2</sub> exchange in Helsinki. In addition, the future CO<sub>2</sub> sinks were projected with the 2050s climate estimated with RCP8.5 scenario. Here, the author was responsible for the design, preparation, and execution of the model simulations. The author wrote the manuscript with contributions from all co-authors.

## References

- Aminipouri, M., Rayner, D., Lindberg, F., Thorsson, S., Knudby, A. J., Zickfeld, K., Middel, A., and Krayenhoff, E. S.: Urban tree planting to maintain outdoor thermal comfort under climate change: The case of Vancouver’s local climate zones, *Building and Environment*, 158, 226–236, <https://doi.org/10.1016/j.buildenv.2019.05.022>, 2019.
- Aubinet, M., Vesala, T., and Papale, D.: Eddy covariance: a practical guide to measurement and data analysis, Springer Science & Business Media, <https://doi.org/10.1007/978-94-007-2351-1>, 2012.
- Baldocchi, D. D.: Assessing the eddy covariance technique for evaluating carbon dioxide exchange rates of ecosystems: past, present and future, *Global change biology*, 9, 479–492, <https://doi.org/10.1046/j.1365-2486.2003.00629.x>, 2003.
- Bechtel, B., Demuzere, M., Mills, G., Zhan, W., Sismanidis, P., Small, C., and Voogt, J.: SUHI analysis using Local Climate Zones-A comparison of 50 cities, *Urban Climate*, 28, 100 451, <https://doi.org/10.1016/j.uclim.2019.01.005>, 2019.
- Bengtsson, L., Andrae, U., Aspelien, T., Batrak, Y., Calvo, J., de Rooy, W., Gleeson, E., Hansen-Sass, B., Homleid, M., Hortal, M., et al.: The HARMONIE–AROME model configuration in the ALADIN–HIRLAM NWP system, *Monthly Weather Review*, 145, 1919–1935, <https://doi.org/10.1175/WAF-D-19-0030.1>, 2017.
- Berland, A., Shiflett, S. A., Shuster, W. D., Garmestani, A. S., Goddard, H. C., Herrmann, D. L., and Hopton, M. E.: The role of trees in urban stormwater management, *Landscape and urban planning*, 162, 167–177, <https://doi.org/10.1016/j.landurbplan.2017.02.017>, 2017.
- Böhm, R.: Urban bias in temperature time series—A case study for the city of Vienna, Austria, *Climatic Change*, 38, 113–128, <https://doi.org/10.1023/A:1005338514333>, 1998.
- Briber, B. M., Hutyrá, L. R., Reinmann, A. B., Raciti, S. M., Dearborn, V. K., Holden, C. E., and Dunn, A. L.: Tree productivity enhanced with conversion from forest to urban land covers, *PLoS One*, 10, e0136 237, <https://doi.org/10.1371/journal.pone.0136237>, 2015.

- Canadell, J. G., Monteiro, P. M., Costa, M. H., Da Cunha, L. C., Cox, P. M., Eliseev, A. V., Henson, S., Ishii, M., Jaccard, S., Koven, C., Lohila, A., Patra, P. K., Piao, S., Rogelj, J., Syampungani, S., Zaehle, S., and Zickfeld, K.: Global carbon and other biogeochemical cycles and feedbacks, *Climate change 2021: The physical science basis. Contribution of working group I to the sixth assessment report of the intergovernmental panel on climate change*, pp. 673–816., <https://doi.org/10.1017/9781009157896.007>, 2021.
- Chang, Q., Xiao, X., Doughty, R., Wu, X., Jiao, W., and Qin, Y.: Assessing variability of optimum air temperature for photosynthesis across site-years, sites and biomes and their effects on photosynthesis estimation, *Agricultural and Forest Meteorology*, 298, 108 277, <https://doi.org/10.1016/j.agrformet.2020.108277>, 2021.
- Christen, A.: Atmospheric measurement techniques to quantify greenhouse gas emissions from cities, *Urban Climate*, 10, 241–260, <https://doi.org/10.1016/j.uclim.2014.04.006>, 2014.
- Christen, A., Emmenegger, L., Hammer, S., Kutsch, W., DâOnofrio, C., Chen, J., Erirt, M., Haeffelin, M., Järvi, L., Kljun, N., et al.: ICOS pilot observatories to monitor greenhouse gas emissions from three different-size European cities, *Copernicus Meetings*, <https://doi.org/10.5194/egusphere-egu23-9884>, 2023.
- Crawford, B., Grimmond, C., and Christen, A.: Five years of carbon dioxide fluxes measurements in a highly vegetated suburban area, *Atmospheric Environment*, 45, 896–905, <https://doi.org/10.1016/j.atmosenv.2010.11.017>, 2011.
- Cucchi, M., Weedon, G., Amici, A., Bellouin, N., Lange, S., Müller Schmied, H., Hersbach, H., Cagnazzo, C., and Buontempo, C.: Near surface meteorological variables from 1979 to 2019 derived from bias-corrected reanalysis, Version 2.0, Copernicus Climate Change Service (C3S) Climate Data Store (CDS) [data set], <https://doi.org/10.24381/cds.20d54e34>, 2021.
- Decina, S. M., Hutyra, L. R., Gately, C. K., Getson, J. M., Reinmann, A. B., Gianotti, A. G. S., and Templer, P. H.: Soil respiration contributes substantially to urban carbon fluxes in the greater Boston area, *Environmental Pollution*, 212, 433–439, <https://doi.org/10.1016/j.envpol.2016.01.012>, 2016.

- Demuzere, M., Bechtel, B., Middel, A., and Mills, G.: Mapping Europe into local climate zones, *PloS one*, 14, e0214474, <https://doi.org/10.1371/journal.pone.0214474>, 2019.
- Demuzere, M., Kittner, J., Martilli, A., Mills, G., Moede, C., Stewart, I. D., van Vliet, J., and Bechtel, B.: Global map of Local Climate Zones, <https://doi.org/10.5281/zenodo.7324909>, 2022.
- Dietrich, F., Chen, J., Voggenreiter, B., Aigner, P., Nachtigall, N., and Reger, B.: MUCCnet: Munich urban carbon column network, *Atmospheric Measurement Techniques*, 14, 1111–1126, <https://doi.org/10.5194/amt-14-1111-2021>, 2021.
- EEA: High Resolution Layer Forest, Dominant Leaf Type 2018, URL <https://land.copernicus.eu/pan-european/high-resolution-layers/forests/dominant-leaf-type/status-maps/dominant-leaf-type-2018>, accessed: 27.06.2023, 2020.
- Flo, V., Martinez-Vilalta, J., Steppe, K., Schuldt, B., and Poyatos, R.: A synthesis of bias and uncertainty in sap flow methods, *Agricultural and Forest Meteorology*, 271, 362–374, <https://doi.org/10.1016/j.agrformet.2019.03.012>, 2019.
- Gál, T., Mahó, S. I., Skarbit, N., and Unger, J.: Numerical modelling for analysis of the effect of different urban green spaces on urban heat load patterns in the present and in the future, *Computers, Environment and Urban Systems*, 87, 101600, <https://doi.org/10.1016/j.compenvurbsys.2021.101600>, 2021.
- Gibelin, A.-L., Calvet, J.-C., and Viovy, N.: Modelling energy and CO<sub>2</sub> fluxes with an interactive vegetation land surface model-Evaluation at high and middle latitudes, *Agricultural and forest meteorology*, 148, 1611–1628, <https://doi.org/10.1016/j.agrformet.2008.05.013>, 2008.
- Goret, M., Masson, V., Schoetter, R., and Moine, M.-P.: Inclusion of CO<sub>2</sub> flux modelling in an urban canopy layer model and an evaluation over an old European city centre, *Atmospheric Environment: X*, 3, 100042, <https://doi.org/10.1016/j.aeaoa.2019.100042>, 2019.
- Granier, A.: Evaluation of transpiration in a Douglas-fir stand by means of sap flow measurements, *Tree physiology*, 3, 309–320, <https://doi.org/10.1093/treephys/3.4.309>, 1987.

- Grimmond, C.: Progress in measuring and observing the urban atmosphere, *Theoretical and Applied Climatology*, 84, 3–22, <https://doi.org/10.1007/s00704-005-0140-5>, 2006.
- Grimmond, C., Oke, T., and Steyn, D.: Urban water balance: 1. A model for daily totals, *Water Resources Research*, 22, 1397–1403, <https://doi.org/10.1029/WR022i010p01397>, 1986.
- Grimmond, C. S. B. and Oke, T. R.: An evapotranspiration-interception model for urban areas, *Water Resources Research*, 27, 1739–1755, <https://doi.org/10.1029/91WR00557>, 1991.
- Hardiman, B. S., Wang, J. A., Hutyra, L. R., Gately, C. K., Getson, J. M., and Friedl, M. A.: Accounting for urban biogenic fluxes in regional carbon budgets, *Science of the Total Environment*, 592, 366–372, <https://doi.org/10.1016/j.scitotenv.2017.03.028>, 2017.
- Hari, P. and Kulmala, L.: *Boreal forest and climate change*, Springer, <https://doi.org/10.1007/978-1-4020-8718-9>, 2008.
- Hersbach, H., Bell, B., Berrisford, P., Hirahara, S., Horányi, A., Muñoz-Sabater, J., Nicolas, J., Peubey, C., Radu, R., Schepers, D., et al.: The ERA5 global re-analysis, *Quarterly Journal of the Royal Meteorological Society*, 146, 1999–2049, <https://doi.org/10.1002/qj.3803>, 2020.
- Hikosaka, K., Ishikawa, K., Borjigidai, A., Muller, O., and Onoda, Y.: Temperature acclimation of photosynthesis: mechanisms involved in the changes in temperature dependence of photosynthetic rate, *Journal of experimental botany*, 57, 291–302, <https://doi.org/10.1093/jxb/erj049>, 2006.
- Hölttä, T., Linkosalo, T., Riikonen, A., Sevanto, S., and Nikinmaa, E.: An analysis of Granier sap flow method, its sensitivity to heat storage and a new approach to improve its time dynamics, *Agricultural and Forest Meteorology*, 211, 2–12, <https://doi.org/10.1016/j.agrformet.2015.05.005>, 2015.
- Huang, F., Jiang, S., Zhan, W., Bechtel, B., Liu, Z., Demuzere, M., Huang, Y., Xu, Y., Ma, L., Xia, W., et al.: Mapping local climate zones for cities: A large review, *Remote Sensing of Environment*, 292, 113573, <https://doi.org/10.1016/j.rse.2023.113573>, 2023.

- Ise, T. and Moorcroft, P. R.: The global-scale temperature and moisture dependencies of soil organic carbon decomposition: an analysis using a mechanistic decomposition model, *Biogeochemistry*, 80, 217–231, <https://doi.org/10.1007/s10533-006-9019-5>, 2006.
- Järvi, L., Hannuniemi, H., Hussein, T., Junninen, H., Aalto, P. P., Hillamo, R., Mäkelä, T., Keronen, P., Siivola, E., Vesala, T., and Kulmala, M.: The urban measurement station SMEAR III: Continuous monitoring of air pollution and surface–atmosphere interactions in Helsinki, Finland, *Boreal Environment Research*, 14, 86–109, 2009.
- Järvi, L., Grimmond, C., and Christen, A.: The surface urban energy and water balance scheme (SUEWS): Evaluation in Los Angeles and Vancouver, *Journal of Hydrology*, 411, 219–237, <https://doi.org/10.1016/j.jhydrol.2011.10.001>, 2011.
- Järvi, L., Nordbo, A., Junninen, H., Riikonen, A., Moilanen, J., Nikinmaa, E., and Vesala, T.: Seasonal and annual variation of carbon dioxide surface fluxes in Helsinki, Finland, in 2006–2010, *Atmospheric Chemistry and Physics*, 12, 8475–8489, <https://doi.org/10.5194/acp-12-8475-2012>, 2012.
- Järvi, L., Grimmond, C. S. B., Taka, M., Nordbo, A., Setälä, H., and Strachan, I. B.: Development of the Surface Urban Energy and Water Balance Scheme (SUEWS) for cold climate cities, *Geoscientific Model Development*, 7, 1691–1711, <https://doi.org/10.5194/gmd-7-1691-2014>, 2014.
- Jarvis, P.: The interpretation of the variations in leaf water potential and stomatal conductance found in canopies in the field, *Philosophical Transactions of the Royal Society of London. B, Biological Sciences*, 273, 593–610, <https://doi.org/10.1098/rstb.1976.0035>, 1976.
- Jokinen, P., Pirinen, P., Kaukoranta, J.-P., Kangas, A., Alenius, P., Eriksson, P., Johansson, M., and Wilkman, S.: Tilastoja Suomen ilmastosta ja merestä 1991–2020, no. 2021:8 in *Ilmatieteen laitoksen raportteja*, Ilmatieteen laitos, Helsinki, <https://doi.org/10.35614/isbn.9789523361485>, 2021.
- Karl, T., Gohm, A., Rotach, M. W., Ward, H. C., Graus, M., Cede, A., Wohlfahrt, G., Hammerle, A., Haid, M., Tiefengraber, M., et al.: Studying urban climate and air quality in the Alps: the Innsbruck atmospheric observatory, *Bulletin of the American Meteorological Society*, 101, E488–E507, <https://doi.org/10.1175/BAMS-D-19-0270.1>, 2020.

- Karsisto, P., Fortelius, C., Demuzere, M., Grimmond, C. S. B., Oleson, K., Kouznetsov, R., Masson, V., and Järvi, L.: Seasonal surface urban energy balance and wintertime stability simulated using three land-surface models in the high-latitude city Helsinki, *Quarterly Journal of the Royal Meteorological Society*, 142, 401–417, <https://doi.org/10.1002/qj.2659>, 2016.
- Karttunen, S., Kurppa, M., Auvinen, M., Hellsten, A., and Järvi, L.: Large-eddy simulation of the optimal street-tree layout for pedestrian-level aerosol particle concentrations—A case study from a city-boulevard, *Atmospheric Environment: X*, 6, 100 073, <https://doi.org/10.1016/j.aeaoa.2020.100073>, 2020.
- Kiel, M., Eldering, A., Roten, D. D., Lin, J. C., Feng, S., Lei, R., Lauvaux, T., Oda, T., Roehl, C. M., Blavier, J.-F., et al.: Urban-focused satellite CO<sub>2</sub> observations from the Orbiting Carbon Observatory-3: A first look at the Los Angeles megacity, *Remote Sensing of Environment*, 258, 112 314, <https://doi.org/10.1016/j.rse.2021.112314>, 2021.
- Kljun, N., Calanca, P., Rotach, M., and Schmid, H.: A simple parameterisation for flux footprint predictions, *Boundary-Layer Meteorology*, 112, 503–523, <https://doi.org/10.1023/B:BOUN.0000030653.71031.96>, 2004.
- Kłysik, K. and Fortuniak, K.: Temporal and spatial characteristics of the urban heat island of Łódź, Poland, *Atmospheric environment*, 33, 3885–3895, [https://doi.org/10.1016/S1352-2310\(99\)00131-4](https://doi.org/10.1016/S1352-2310(99)00131-4), 1999.
- Kokkonen, T., Grimmond, C., Christen, A., Oke, T., and Järvi, L.: Changes to the water balance over a century of urban development in two neighborhoods: Vancouver, Canada, *Water Resources Research*, 54, 6625–6642, <https://doi.org/10.1029/2017WR022445>, 2018.
- Kokkonen, T. V., Grimmond, S., Murto, S., Liu, H., Sundström, A.-M., and Järvi, L.: Simulation of the radiative effect of haze on the urban hydrological cycle using reanalysis data in Beijing, *Atmospheric Chemistry and Physics*, 19, 7001–7017, <https://doi.org/10.5194/acp-19-7001-2019>, 2019.
- Korhonen, K. T., Ihalainen, A., Packalen, T., Salminen, O., Hirvelä, H., and Härkönen, K.: Uudenmaan metsävarat ja hakkuumahdollisuudet (in Finnish), Luonnonvarakeskus (LUKE) reports, 2015.

- Kunert, N., Hajek, P., Hietz, P., Morris, H., Rosner, S., and Tholen, D.: Summer temperatures reach the thermal tolerance threshold of photosynthetic decline in temperate conifers, *Plant Biology*, 24, 1254–1261, <https://doi.org/10.1111/plb.13349>, 2022.
- Launiainen, S., Katul, G. G., Lauren, A., and Kolari, P.: Coupling boreal forest CO<sub>2</sub>, H<sub>2</sub>O and energy flows by a vertically structured forest canopy–Soil model with separate bryophyte layer, *Ecological Modelling*, 312, 385–405, <https://doi.org/10.1016/j.ecolmodel.2015.06.007>, 2015.
- Lian, J., Lauvaux, T., Utard, H., Bréon, F.-M., Broquet, G., Ramonet, M., Laurent, O., Albarus, I., Chariot, M., Kotthaus, S., et al.: Can we use atmospheric CO<sub>2</sub> measurements to verify emission trends reported by cities? Lessons from a six-year atmospheric inversion over Paris, *EGU sphere*, 2023, 1–15, <https://doi.org/10.5194/acp-23-8823-2023>, 2023.
- Lindberg, F., Grimmond, C. S. B., Gabey, A., Huang, B., Kent, C. W., Sun, T., Theeuwes, N. E., Järvi, L., Ward, H. C., Capel-Timms, I., et al.: Urban Multi-scale Environmental Predictor (UMEP): An integrated tool for city-based climate services, *Environmental Modelling & Software*, 99, 70–87, <https://doi.org/10.1016/j.envsoft.2017.09.020>, 2018.
- Lindén, L., Riikonen, A., Setälä, H., and Yli-Pelkonen, V.: Quantifying carbon stocks in urban parks under cold climate conditions, *Urban Forestry & Urban Greening*, 49, 126–133, <https://doi.org/10.1016/j.ufug.2020.126633>, 2020.
- Liski, J., Palosuo, T., Peltoniemi, M., and Sievänen, R.: Carbon and decomposition model Yasso for forest soils, *Ecological Modelling*, 189, 168–182, <https://doi.org/10.1016/j.ecolmodel.2005.03.005>, 2005.
- Liski, J., Lehtonen, A., Palosuo, T., Peltoniemi, M., Eggers, T., Muukkonen, P., and Mäkipää, R.: Carbon accumulation in Finland’s forests 1922–2004—an estimate obtained by combination of forest inventory data with modelling of biomass, litter and soil, *Annals of Forest Science*, 63, 687–697, <https://doi.org/10.1051/forest:2006049>, 2006.
- Liu, H., Feng, J., Järvi, L., and Vesala, T.: Four-year (2006–2009) eddy covariance measurements of CO<sub>2</sub> flux over an urban area in Beijing, *Atmospheric Chemistry and Physics*, 12, 7881–7892, <https://doi.org/10.5194/acp-12-7881-2012>, 2012.

- Liu, P., Zha, T., Zhang, F., Jia, X., Bourque, C. P.-A., Tian, Y., Bai, Y., Yang, R., Li, X., Yu, H., et al.: Environmental controls on carbon fluxes in an urban forest in the Megalopolis of Beijing, 2012-2020, *Agricultural and Forest Meteorology*, 333, 109 412, <https://doi.org/10.1016/j.agrformet.2023.109412>, 2023.
- Livesley, S. J., Dougherty, B. J., Smith, A. J., Navaud, D., Wylie, L. J., and Arndt, S. K.: Soil-atmosphere exchange of carbon dioxide, methane and nitrous oxide in urban garden systems: impact of irrigation, fertiliser and mulch, *Urban ecosystems*, 13, 273–293, <https://doi.org/10.1007/s11252-009-0119-6>, 2010.
- Livingston, G. and Hutchinson, G.: Enclosure-based measurement of trace gas exchange: applications and sources of error, *Biogenic trace gases: measuring emissions from soil and water*, 51, 14–50, 1995.
- Lwasa, S., Seto, K., Bai, X., Blanco, H., Gurney, K., Kilkis, S., Lucon, O., Murakami, J., Pan, J., Sharifi, A., et al.: Urban systems and other settlements, *Climate Change 2022: Mitigation of Climate Change. Contribution of Working Group III to the Sixth Assessment Report of the Intergovernmental Panel on Climate Change*, <https://doi.org/10.1017/9781009157926.010>, 2022.
- Melaas, E. K., Wang, J. A., Miller, D. L., and Friedl, M. A.: Interactions between urban vegetation and surface urban heat islands: a case study in the Boston metropolitan region, *Environmental Research Letters*, 11, 054 020, <https://doi.org/10.1088/1748-9326/11/5/054020>, 2016.
- Menzer, O. and McFadden, J. P.: Statistical partitioning of a three-year time series of direct urban net CO<sub>2</sub> flux measurements into biogenic and anthropogenic components, *Atmospheric Environment*, 170, 319–333, <https://doi.org/10.1016/j.atmosenv.2017.09.049>, 2017.
- Menzer, O., Meiring, W., Kyriakidis, P. C., and McFadden, J. P.: Annual sums of carbon dioxide exchange over a heterogeneous urban landscape through machine learning based gap-filling, *Atmospheric Environment*, 101, 312–327, <https://doi.org/10.1016/j.atmosenv.2014.11.006>, 2015.
- Mirzaei, P. A.: Recent challenges in modeling of urban heat island, *Sustainable cities and society*, 19, 200–206, <https://doi.org/10.1016/j.scs.2015.04.001>, 2015.

- Mirzaei, P. A. and Haghghat, F.: Approaches to study urban heat island–abilities and limitations, *Building and environment*, 45, 2192–2201, <https://doi.org/10.1016/j.buildenv.2010.04.001>, 2010.
- Mitchell, L. E., Lin, J. C., Hutyra, L. R., Bowling, D. R., Cohen, R. C., Davis, K. J., DiGangi, E., Duren, R. M., Ehleringer, J. R., Fain, C., et al.: A multi-city urban atmospheric greenhouse gas measurement data synthesis, *Scientific Data*, 9, 361, <https://doi.org/10.1038/s41597-022-01467-3>, 2022.
- Monteith, J. L.: Evaporation and environment, in: *Symposia of the society for experimental biology*, vol. 19, pp. 205–234, Cambridge University Press (CUP) Cambridge, 1965.
- Mouzourides, P., Eleftheriou, A., Kyprianou, A., Ching, J., and Neophytou, M. K.-A.: Linking local-climate-zones mapping to multi-resolution-analysis to deduce associative relations at intra-urban scales through an example of Metropolitan London, *Urban Climate*, 30, 100 505, <https://doi.org/10.1016/j.uclim.2019.100505>, 2019.
- Müller, M., Homleid, M., Ivarsson, K.-I., Køltzow, M. A., Lindskog, M., Midtbø, K. H., Andrae, U., Aspelien, T., Berggren, L., Bjørge, D., et al.: AROME-MetCoOp: A Nordic convective-scale operational weather prediction model, *Weather and Forecasting*, 32, 609–627, <https://doi.org/10.1175/WAF-D-16-0099.1>, 2017.
- Nielsen, C. N., Buhler, O., and Kristoffersen, P.: Soil Water Dynamics and Growth of Street and Park Trees, *Arboriculture and Urban Forestry*, 33, 231, <https://doi.org/10.48044/jauf.2007.027>, 2007.
- Nipen, T. N., Seierstad, I. A., Lussana, C., Kristiansen, J., and Hov, Ø.: Adopting citizen observations in operational weather prediction, *Bulletin of the American Meteorological Society*, 101, E43–E57, <https://doi.org/10.1175/BAMS-D-18-0237.1>, 2020.
- Niu, S., Luo, Y., Fei, S., Yuan, W., Schimel, D., Law, B. E., Ammann, C., Altaf Arain, M., Arneth, A., Aubinet, M., et al.: Thermal optimality of net ecosystem exchange of carbon dioxide and underlying mechanisms, *New Phytologist*, 194, 775–783, <https://doi.org/10.1111/j.1469-8137.2012.04095.x>, 2012.
- Nordbo, A., Järvi, L., Haapanala, S., Wood, C. R., and Vesala, T.: Fraction of natural area as main predictor of net CO<sub>2</sub> emissions from cities, *Geophysical Research Letters*, 39, <https://doi.org/10.1029/2012GL053087>, 2012a.

- Nordbo, A., Järvi, L., and Vesala, T.: Revised eddy covariance flux calculation methodologies—effect on urban energy balance, *Tellus B: Chemical and Physical Meteorology*, 64, 18184, <https://doi.org/10.3402/tellusb.v64i0.18184>, 2012b.
- Nordbo, A., Järvi, L., Haapanala, S., Moilanen, J., and Vesala, T.: Intra-city variation in urban morphology and turbulence structure in Helsinki, Finland, *Boundary-layer meteorology*, 146, 469–496, <https://doi.org/10.1007/s10546-012-9773-y>, 2013.
- Nordbo, A., Karsisto, P., Matikainen, L., Wood, C. R., and Järvi, L.: Urban surface cover determined with airborne lidar at 2 m resolution—implications for surface energy balance modelling, *Urban Climate*, 13, 52–72, <https://doi.org/10.1016/j.uclim.2015.05.004>, 2015.
- Novick, K. A., Ficklin, D. L., Stoy, P. C., Williams, C. A., Bohrer, G., Oishi, A. C., Papuga, S. A., Blanken, P. D., Noormets, A., Sulman, B. N., et al.: The increasing importance of atmospheric demand for ecosystem water and carbon fluxes, *Nature climate change*, 6, 1023–1027, <https://doi.org/10.1038/nclimate3114>, 2016.
- Nowak, D. J. and Crane, D. E.: The Urban Forest Effects (UFORE) Model: quantifying urban forest structure and functions, In: Hansen, Mark; Burk, Tom, eds. *Integrated tools for natural resources inventories in the 21st century*. Gen. Tech. Rep. NC-212. St. Paul, MN: US Dept. of Agriculture, Forest Service, North Central Forest Experiment Station. 714-720., 212, 2000.
- Nowak, R. S., Ellsworth, D. S., and Smith, S. D.: Functional responses of plants to elevated atmospheric CO<sub>2</sub>—do photosynthetic and productivity data from FACE experiments support early predictions?, *New phytologist*, 162, 253–280, <https://doi.org/10.1111/j.1469-8137.2004.01033.x>, 2004.
- Offerle, B., Grimmond, C., and Oke, T. R.: Parameterization of net all-wave radiation for urban areas, *Journal of Applied Meteorology and Climatology*, 42, 1157–1173, [https://doi.org/10.1175/1520-0450\(2003\)042<1157:PONARF>2.0.CO;2](https://doi.org/10.1175/1520-0450(2003)042<1157:PONARF>2.0.CO;2), 2003.
- Ogink-Hendriks, M.: Modelling surface conductance and transpiration of an oak forest in The Netherlands, *Agricultural and Forest Meteorology*, 74, 99–118, [https://doi.org/10.1016/0168-1923\(94\)02180-R](https://doi.org/10.1016/0168-1923(94)02180-R), 1995.
- Oke, T. R.: The energetic basis of the urban heat island, *Quarterly Journal of the Royal Meteorological Society*, 108, 1–24, <https://doi.org/10.1002/qj.49710845502>, 1982.

- Oke, T. R., Mills, G., Christen, A., and Voogt, J. A.: Urban climates, Cambridge University Press, <https://doi.org/10.1017/9781139016476>, 2017.
- Penman, H. L.: Natural evaporation from open water, bare soil and grass, *Proceedings of the Royal Society of London. Series A. Mathematical and Physical Sciences*, 193, 120–145, <https://doi.org/10.1098/rspa.1948.0037>, 1948.
- Poyatos, R., Granda, V., Flo, V., Adams, M. A., Adorján, B., Aguadé, D., Aidar, M. P., Allen, S., Alvarado-Barrientos, M. S., Anderson-Teixeira, K. J., et al.: Global transpiration data from sap flow measurements: the SAPFLUXNET database, *Earth System Science Data Discussions*, 2020, 1–57, <https://doi.org/10.5194/essd-13-2607-2021>, 2020.
- Pumpanen, J., Kulmala, L., Linden, A., Kolari, P., Nikinmaa, E., and Hari, P.: Seasonal dynamics of autotrophic respiration in boreal forest soil estimated by continuous chamber measurements, 2015.
- Rahman, M. A., Stratopoulos, L. M., Moser-Reischl, A., Zölch, T., Häberle, K.-H., Rötzer, T., Pretzsch, H., and Pauleit, S.: Traits of trees for cooling urban heat islands: A meta-analysis, *Building and Environment*, 170, 106606, <https://doi.org/10.1016/j.buildenv.2019.106606>, 2020.
- Rathnayake, N., Perera, N., and Emmanuel, M.: Anthropogenic heat implications of Colombo core area development plan, in: *IOP Conference Series: Earth and Environmental Science*, vol. 471, p. 012002, IOP Publishing, <https://doi.org/10.1088/1755-1315/471/1/012002>, 2020.
- Reich, P. B., Sendall, K. M., Stefanski, A., Rich, R. L., Hobbie, S. E., and Montgomery, R. A.: Effects of climate warming on photosynthesis in boreal tree species depend on soil moisture, *Nature*, 562, 263–267, <https://doi.org/10.1038/s41586-018-0582-4>, 2018.
- Riikonen, A., Lindén, L., Pulkkinen, M., and Nikinmaa, E.: Post-transplant crown allometry and shoot growth of two species of street trees, *Urban Forestry & Urban Greening*, 10, 87–94, <https://doi.org/10.1016/j.ufug.2010.09.001>, 2011.
- Riikonen, A., Järvi, L., and Nikinmaa, E.: Environmental and crown related factors affecting street tree transpiration in Helsinki, Finland, *Urban Ecosystems*, 19, 1693–1715, <https://doi.org/10.1007/s11252-016-0561-1>, 2016.

- Riikonen, A., Pumpanen, J., Mäki, M., and Nikinmaa, E.: High carbon losses from established growing sites delay the carbon sequestration benefits of street tree plantings—A case study in Helsinki, Finland, *Urban Forestry & Urban Greening*, 26, 85–94, <https://doi.org/10.1016/j.ufug.2017.04.004>, 2017.
- Russo, A., Escobedo, F. J., Timilsina, N., Schmitt, A. O., Varela, S., and Zerbe, S.: Assessing urban tree carbon storage and sequestration in Bolzano, Italy, *International Journal of Biodiversity Science, Ecosystem Services & Management*, 10, 54–70, <https://doi.org/10.1080/21513732.2013.873822>, 2014.
- Ryan, M. G., Lavigne, M. B., and Gower, S. T.: Annual carbon cost of autotrophic respiration in boreal forest ecosystems in relation to species and climate, *Journal of Geophysical Research: Atmospheres*, 102, 28 871–28 883, <https://doi.org/10.1029/97JD01236>, 1997.
- Sabbatini, S., Mammarella, I., Arriga, N., Fratini, G., Graf, A., Hoertriagl, L., Ibrom, A., Longdoz, B., Mauder, M., Merbold, L., et al.: Eddy covariance raw data processing for CO<sub>2</sub> and energy fluxes calculation at ICOS ecosystem stations, *International Agrophysics*, <https://doi.org/10.1515/intag-2017-0043>, 2018.
- Sage, R. F., Way, D. A., and Kubien, D. S.: Rubisco, Rubisco activase, and global climate change, *Journal of experimental botany*, 59, 1581–1595, <https://doi.org/10.1093/jxb/ern053>, 2008.
- Salvia, M., Reckien, D., Pietrapertosa, F., Eckersley, P., Spyridaki, N.-A., Krook-Riekkola, A., Olazabal, M., Hurtado, S. D. G., Simoes, S. G., Geneletti, D., et al.: Will climate mitigation ambitions lead to carbon neutrality? An analysis of the local-level plans of 327 cities in the EU, *Renewable and Sustainable Energy Reviews*, 135, 110 253, <https://doi.org/10.1016/j.rser.2020.110253>, 2021.
- Santamouris, M.: Heat island research in Europe: the state of the art, *Advances in building energy research*, 1, 123–150, <https://doi.org/10.1080/17512549.2007.9687272>, 2007.
- Saranko, O., Fortelius, C., Jylhä, K., Ruosteenoja, K., Brattich, E., Di Sabatino, S., and Nurmi, V.: Impacts of town characteristics on the changing urban climate in Vantaa, *Science of The Total Environment*, 727, 138 471, <https://doi.org/10.1016/j.scitotenv.2020.138471>, 2020.

- Schuh, A. E., Otte, M., Lauvaux, T., and Oda, T.: Far-field biogenic and anthropogenic emissions as a dominant source of variability in local urban carbon budgets: A global high-resolution model study with implications for satellite remote sensing, *Remote Sensing of Environment*, 262, 112473, <https://doi.org/10.1016/j.rse.2021.112473>, 2021.
- Schulze, E. D., Čermák, J., Matyssek, M., Penka, M., Zimmermann, R., Vasicek, F., Gries, W., and Kučera, J.: Canopy transpiration and water fluxes in the xylem of the trunk of *Larix* and *Picea* trees—a comparison of xylem flow, porometer and cuvette measurements, *Oecologia*, 66, 475–483, <https://doi.org/10.1007/BF00379337>, 1985.
- Shi, Y., Ren, C., Lau, K. K.-L., and Ng, E.: Investigating the influence of urban land use and landscape pattern on PM<sub>2.5</sub> spatial variation using mobile monitoring and WUDAPT, *Landscape and urban planning*, 189, 15–26, 2019.
- Soares, A. L., Rego, F. C., McPherson, E., Simpson, J., Peper, P., and Xiao, Q.: Benefits and costs of street trees in Lisbon, Portugal, *Urban Forestry & Urban Greening*, 10, 69–78, <https://doi.org/10.1016/j.ufug.2010.12.001>, 2011.
- Stagakis, S., Feigenwinter, C., Vogt, R., Brunner, D., and Kalberer, M.: A high-resolution monitoring approach of urban CO<sub>2</sub> fluxes. Part 2—surface flux optimisation using eddy covariance observations, *Science of The Total Environment*, 903, 166035, <https://doi.org/10.1016/j.scitotenv.2023.166035>, 2023a.
- Stagakis, S., Feigenwinter, C., Vogt, R., and Kalberer, M.: A high-resolution monitoring approach of urban CO<sub>2</sub> fluxes. Part 1—bottom-up model development, *Science of The Total Environment*, 858, 160216, <https://doi.org/10.1016/j.scitotenv.2022.160216>, 2023b.
- Stewart, I. D. and Oke, T. R.: Local climate zones for urban temperature studies, *Bulletin of the American Meteorological Society*, 93, 1879–1900, <https://doi.org/10.1175/BAMS-D-11-00019.1>, 2012.
- Stewart, I. D., Oke, T. R., and Krayenhoff, E. S.: Evaluation of the local climate zone scheme using temperature observations and model simulations, *International journal of climatology*, 34, 1062–1080, <https://doi.org/10.1002/joc.3746>, 2014.
- Stewart, J.: Modelling surface conductance of pine forest, *Agricultural and Forest meteorology*, 43, 19–35, [https://doi.org/10.1016/0168-1923\(88\)90003-2](https://doi.org/10.1016/0168-1923(88)90003-2), 1988.

- StromJan: StromJan/Raster4H: Final version, <https://doi.org/10.5281/zenodo.4005833>, 2020.
- Stull, R. B.: An introduction to boundary layer meteorology, vol. 13, Springer Science & Business Media, 1988.
- Sun, T., Wang, Z.-H., Oechel, W. C., and Grimmond, S.: The Analytical Objective Hysteresis Model (AnOHM v1. 0): methodology to determine bulk storage heat flux coefficients, *Geoscientific Model Development*, 10, 2875–2890, <https://doi.org/10.5194/gmd-10-2875-2017>, 2017.
- Tang, Y., Sun, T., Luo, Z., Omidvar, H., Theeuwes, N., Xie, X., Xiong, J., Yao, R., and Grimmond, S.: Urban meteorological forcing data for building energy simulations, *Building and Environment*, 204, 108 088, <https://doi.org/10.1016/j.buildenv.2021.108088>, 2021.
- Taylor, G., Tallis, M. J., Giardina, C. P., Percy, K. E., Miglietta, F., Gupta, P. S., Gioli, B., Calfapietra, C., Gielen, B., Kubiske, M. E., et al.: Future atmospheric CO<sub>2</sub> leads to delayed autumnal senescence, *Global Change Biology*, 14, 264–275, <https://doi.org/10.1111/j.1365-2486.2007.01473.x>, 2008.
- Tse, J. W. P., Yeung, P. S., Fung, J. C.-H., Ren, C., Wang, R., Wong, M. M.-F., and Meng, C.: Investigation of the meteorological effects of urbanization in recent decades: A case study of major cities in Pearl River Delta, *Urban climate*, 26, 174–187, <https://doi.org/10.1016/j.uclim.2018.08.007>, 2018.
- Tuomi, M., Thum, T., Järvinen, H., Fronzek, S., Berg, B., Harmon, M., Trofymow, J., Sevanto, S., and Liski, J.: Leaf litter decomposition—Estimates of global variability based on Yasso07 model, *Ecological Modelling*, 220, 3362–3371, <https://doi.org/10.1016/j.ecolmodel.2009.05.016>, 2009.
- Tuomi, M., Rasinmäki, J., Repo, A., Vanhala, P., and Liski, J.: Soil carbon model Yasso07 graphical user interface, *Environmental Modelling & Software*, 26, 1358–1362, <https://doi.org/10.1016/j.envsoft.2011.05.009>, 2011.
- UN: World urbanization prospects the 2018 revision, Population Division, Department of Economic and Social Affairs, United Nations, New York, 2019.
- Vaccari, F. P., Gioli, B., Toscano, P., and Perrone, C.: Carbon dioxide balance assessment of the city of Florence (Italy), and implications for urban planning, *Landscape*

- and Urban Planning, 120, 138–146, <https://doi.org/10.1016/j.landurbplan.2013.08.004>, 2013.
- Velasco, E., Roth, M., Norford, L., and Molina, L. T.: Does urban vegetation enhance carbon sequestration?, *Landscape and urban planning*, 148, 99–107, <https://doi.org/10.1016/j.landurbplan.2015.12.003>, 2016.
- Velasco, E., Segovia, E., Choong, A. M., Lim, B. K., and Vargas, R.: Carbon dioxide dynamics in a residential lawn of a tropical city, *Journal of Environmental Management*, 280, 111 752, <https://doi.org/10.1016/j.jenvman.2020.111752>, 2021.
- Verdonck, M.-L., Demuzere, M., Hooyberghs, H., Priem, F., and Van Coillie, F.: Heat risk assessment for the Brussels capital region under different urban planning and greenhouse gas emission scenarios, *Journal of environmental management*, 249, 109 210, <https://doi.org/10.1016/j.jenvman.2019.06.111>, 2019.
- Vesala, T., Järvi, L., Launiainen, S., Sogachev, A., Rannik, Ü., Mammarella, I., Ivola, E. S., Keronen, P., Rinne, J., Riikonen, A., et al.: Surface–atmosphere interactions over complex urban terrain in Helsinki, Finland, *Tellus B: Chemical and Physical Meteorology*, 60, 188–199, <https://doi.org/10.1111/j.1600-0889.2007.00312.x>, 2008.
- Viskari, T., Laine, M., Kulmala, L., Mäkelä, J., Fer, I., and Liski, J.: Improving Yasso15 soil carbon model estimates with ensemble adjustment Kalman filter state data assimilation, *Geoscientific Model Development*, 13, 5959–5971, <https://doi.org/10.5194/gmd-13-5959-2020>, 2020.
- Vogt, R., Christen, A., Rotach, M., Roth, M., and Satyanarayana, A.: Temporal dynamics of CO<sub>2</sub> fluxes and profiles over a Central European city, *Theoretical and applied climatology*, 84, 117–126, <https://doi.org/10.1007/s00704-005-0149-9>, 2006.
- Wang, J., Xiang, Z., Wang, W., Chang, W., and Wang, Y.: Impacts of strengthened warming by urban heat island on carbon sequestration of urban ecosystems in a subtropical city of China, *Urban Ecosystems*, 24, 1165–1177, <https://doi.org/10.1007/s11252-021-01104-8>, 2021.
- Ward, H., Kotthaus, S., Grimmond, C., BJORKEGREN, A., Wilkinson, M., Morrison, W., Evans, J., Morison, J., and Iamarino, M.: Effects of urban density on carbon dioxide exchanges: Observations of dense urban, suburban and woodland areas of southern England, *Environmental Pollution*, 198, 186–200, <https://doi.org/10.1016/j.envpol.2014.12.031>, 2015.

- Ward, H. C., Kotthaus, S., Järvi, L., and Grimmond, C. S. B.: Surface Urban Energy and Water Balance Scheme (SUEWS): development and evaluation at two UK sites, *Urban Climate*, 18, 1–32, <https://doi.org/10.1016/j.uclim.2016.05.001>, 2016.
- Wei, D., Reinmann, A., Schiferl, L. D., and Commane, R.: High resolution modeling of vegetation reveals large summertime biogenic CO<sub>2</sub> fluxes in New York City, *Environmental Research Letters*, 17, 124 031, <https://doi.org/10.1088/1748-9326/aca68f>, 2022.
- Weissert, L., Salmond, J., and Schwendenmann, L.: A review of the current progress in quantifying the potential of urban forests to mitigate urban CO<sub>2</sub> emissions, *Urban Climate*, 8, 100–125, <https://doi.org/10.1016/j.uclim.2014.01.002>, 2014.
- Weissert, L., Salmond, J., and Schwendenmann, L.: Variability of soil organic carbon stocks and soil CO<sub>2</sub> efflux across urban land use and soil cover types, *Geoderma*, 271, 80–90, <https://doi.org/10.1016/j.geoderma.2016.02.014>, 2016a.
- Weissert, L., Salmond, J., Turnbull, J., and Schwendenmann, L.: Temporal variability in the sources and fluxes of CO<sub>2</sub> in a residential area in an evergreen subtropical city, *Atmospheric Environment*, 143, 164–176, <https://doi.org/10.1016/j.atmosenv.2016.08.044>, 2016b.
- Winbourne, J. B., Jones, T. S., Garvey, S. M., Harrison, J. L., Wang, L., Li, D., Templer, P. H., and Hutyrá, L.: Tree transpiration and urban temperatures: current understanding, implications, and future research directions, *BioScience*, 70, 576–588, <https://doi.org/10.1093/biosci/biaa055>, 2020.
- Wolf, K. L., Lam, S. T., McKeen, J. K., Richardson, G. R., Van Den Bosch, M., and Bardekjian, A. C.: Urban trees and human health: A scoping review, *International journal of environmental research and public health*, 17, 4371, <https://doi.org/10.3390/ijerph17124371>, 2020.
- Wu, Y., Sharifi, A., Yang, P., Borjigin, H., Murakami, D., and Yamagata, Y.: Mapping building carbon emissions within local climate zones in Shanghai, *Energy Procedia*, 152, 815–822, <https://doi.org/10.1016/j.egypro.2018.09.195>, 2018.
- Zhao, S., Liu, S., and Zhou, D.: Prevalent vegetation growth enhancement in urban environment, *Proceedings of the National Academy of Sciences*, 113, 6313–6318, <https://doi.org/10.1073/pnas.1602312113>, 2016.